Faculty of Science and Engineering

Department of Civil Engineering

An Assessment of the Asphalt Fatigue Equation for Bitumen Stabilised Materials

Ethan Dadras

This thesis is presented for the Degree of

Master of Philosophy

Of

Curtin University

September 2016

DECLARATION

To the best of my knowledge and belief, this thesis contains no material previously published by any other person except where due acknowledgement has been made. This thesis contains no material that has been accepted for the award of any other degree or diploma in any university.

Date:.....19/01/2017.....

TABLE OF CONTENTS

LIST OF FIGURES

ACKNOWLEDGEMENT

This thesis is part of a research project on an investigation into the fatigue parameters of stabilised pavement. The research has been carried out at Curtin University. I would like to acknowledge and thank my supervisor Professor Hamid Nikraz from Curtin University who inspired me to continue with this research and has constantly provided encouragement, enthusiasm, and support throughout this study program.

As well as my supervisor I would like to thank Hossein Asadi as my mentor from ARRB Group Ltd who inspired me and has willingly provided with information and helped me to conclude this research.

I would also like to thank Mr Darren Issac from Curtin University Geomechanical Laboratory.

Finally my sincere thanks to the family and friends especially my wife Nina that her support and encouragement helped me to continue my studies.

SUMMARY

The basis for the Austroads method for the design of in-situ foamed bitumen stabilised pavements is that the fatigue life of the pavement can be predicted using the same asphalt fatigue equation as applied in the Austroads Guide to Pavement Technology Part 2, Structural Design. However, the use of this formula can result in the fatigue life being predicted shorter or longer than reality, which is an issue of concern to the industry. This is particularly relevant, as the process of asphalt manufacture results in an entirely different bitumen distribution to that achieved in the foamed bitumen stabilisation process.

The fatigue equation was published by Shell (Shell, 1978) Reliability factors are applied to the fatigue equation that relates the laboratory tests to the practical in-service situation for asphalt. Based on a road classification, the Reliability factors could be chosen between 2.5 to 0.67 as suggested in section 2.2.1 of Austroads Guide to pavement technology part 2: pavement structural design, AGPT2 (Austroads, 2012). However, it is notable that the original basis of the Shell method was based on isotropic subgrade (Shell, 1978) and granular behaviour whereas the Austroads methods assume anisotropic behaviour.

The aim of this research is to investigate the laboratory fatigue performance of a typical foamed bitumen mix used in Western Australia to validate if Austroads fatigue equation is applicable to the design of in-situ foamed bitumen stabilised materials. A new four-point bending device was utilised as a scaled up version which allows testing of much larger beams by removing the constraint that the maximum width and thickness are dominated by maximum aggregate size. This device is able to test beams with dimensions of up to 800 mm long, 160 mm thick and 200 mm wide.

A range of Western Australian foamed bitumen stabilised base course samples extracted from actual road projects and cut to the approximate dimension of 800 mm × 150 mm × 200 mm for testing in the laboratory. The main focus of this study was placed on assessing the validity of asphalt fatigue relationship provided in AGPT2 (Austroads, 2012) for foamed bitumen stabilised materials.

Following the laboratory fatigue testing of the beams, it was concluded that the asphalt fatigue equation is not suitable for in-situ foamed stabilised materials.

1. INTRODUCTION

1.1 Background

Based on CSIR Transportek's Mix Design Procedure, Dr Ladi H Csanyi at the Engineering Experiment Station in Iowa State University first realised the potential of using foamed bitumen in 1956. Since then, foamed bitumen technology has been developed and used in many countries. In1968 Mobil Oil Australia modified the original process by adding cold water rather than steam into the hot bitumen. (Kendall, et al., 1999).

In Australia, following the great expansion of the sealed road network in the 1960's and 70's, the maintenance and rehabilitation costs of road network have been increased, and each year road agencies in Australia spending above $20 billions of dollars managing their roads (Government, 2009).

Historically, empirical methods have been used to design flexible pavements with thin surfacings over unbound granular materials in Australia based on the experimental chart known as Figure 8.4 provided in the current AGPT02 (Austroads, 2012). The fundamental drawback of this approach is that it does not consider the material properties of base and subbase and the failure modes within these layers and the main objective is to provide sufficient thickness to limit subgrade strain. Mechanistic-empirical (ME) methods were developed to fill this gap and to predict the performance of bound layers in a pavement but still did not consider the failure of the granular pavement materials. In this approach, factors are applied to relate laboratory performance to field observations of performance and reliability factors applied to relate risk of failures to road class.

With the demands placed on the existing road network by ever increasing traffic volumes, greater tyre pressures and heavier axle loads, the importance for determining the optimum whole of life solution for pavements that are no longer fit for purpose is essential to asset managers. These pavements may require rehabilitation due to poor initial design, poor material selection, or changes in traffic characteristics compared to that at the time of construction.

One method of rehabilitation which has been used widely in recent years is the in situ foamed bitumen stabilisation process. The fatigue life of foamed bitumen stabilised material in Australia is generally predicted using the following asphalt fatigue equation (Equation 1-1) provided in the AGPT02 (Austroads, 2012):

$$N = RF\left[\frac{6918(0.856V_b + 1.08)}{S_{mix}{}^{0.36}\,\mu\varepsilon}\right]^5 \qquad 1\text{-}1$$

Where:

N = Allowable number of load repetitions

$\mu\varepsilon$ = the tensile strain produced by a single load repetition

V_b = percentage of bitumen by volume

S_{mix} = modulus of the stabilised material

RF = reliability factor for asphalt fatigue

In flexible pavements, fatigue cracking occurs when repeated traffic loads induce tensile strain at the bottom of asphalt layer (Figure 1-1). Factors that can influence the pavement's ability to withstand fatigue could be categorised as follows:

- Pavement structure,
- the age of the pavement and the materials used in construction,
- the magnitude of loading (load and numbers of vehicles),
- the speed of loading,
- and temperature.

The four-point bending beam fatigue test is normally used to investigate fatigue performance of hot mixed asphalt in Australia. Overestimating the asphalt fatigue life could lead to a flexible pavement design such that asphalt will fatigue under traffic loading earlier than anticipated. Conversely underestimation of the fatigue life could lead to costly design.

Figure 1-1: Extensive fatigue cracking (Pavementinteractive, 2011)

Whilst the above applies to asphalt where a considerable amount of data is available, the assumptions applied to foamed bitumen stabilised pavements has historically been assumed to apply in Australia (Leek, 2002). However, where asphalt is manufactured in a plant and all aggregates are heated to high temperatures and fully coated with bitumen, the same does not apply to foamed bitumen, where nodules of bitumen are assumed to spot weld larger particles (Jenkins, et al., 1999). In situ foamed bitumen is not homogeneous, so, the bitumen film is discontinuous and distributed as discrete droplets around fines in the mix (Leek, et al., 2014).

The fatigue life of pavement materials in the laboratory is determined using the four-point bending beam apparatus which requires beams to be cut to a size of 50 mm × 62 mm × 400 mm. However, questions are raised about the validity of using this device to test materials where aggregate sizes are larger than 50 mm (Leek, 2002).

To test the fatigue performance of materials containing large aggregates, Curtin University commissioned IPC Global to develop a large four-point bending beam apparatus as a scaled up version of the currently used device. This device can test beams of up to 800 mm long, 160 mm thick and 200 mm wide.

Hence, this research was initiated to address the abovementioned issues and enable the design of in-situ foamed bitumen stabilised pavements to be undertaken with greater confidence utilising the potential of the new large four-point flexural beam apparatus.

The aim of this research is to assess whether the asphalt fatigue equation defined in Equation 1-1 is applicable to in-situ foamed bitumen stabilised materials or not.

1.2 Experimental Investigations

The materials used to provide data for this research was obtained from samples collected from Nicholson Road in Canning Vale in the City of Canning. Large slabs were extracted from the pavement and delivered to Curtin University. These slabs were then further cut to size and 14 beams were obtained. These beams were tested at the Geomechanical Laboratory at Curtin University in the large four-point bending beam apparatus as shown in Figure 1-2 at controlled strain and temperature mode. A schematic diagram also provided in Figure 1-3. A total of 14 tests were undertaken over a range of three strain levels and one temperature of 20ºC.

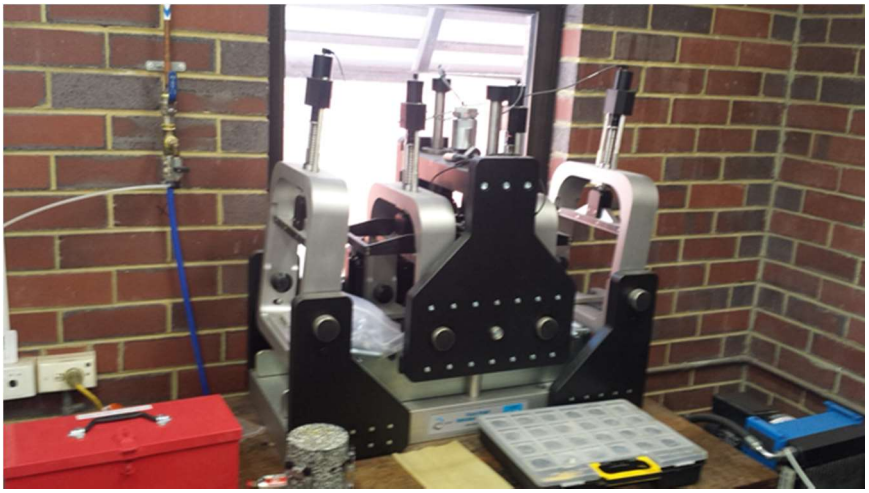

Figure 1-2: Large four-point bending beam apparatus

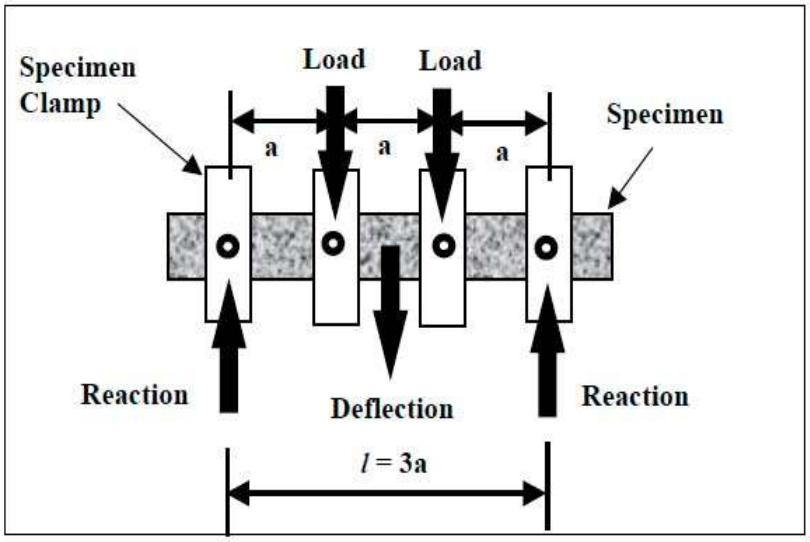

Figure 1-3: Schematic diagram of four-point bending beam (Al-Khateeb, 2008)

To enable comparison between the estimated fatigue lives from standard four-point bending

beam apparatus and extra-large four-point bending beam machine, data provided in Australian Road Research Board (ARRB) transport research report was reviewed. The design information for Nicholson Road pavement from ARRB transport report is shown in Table 1-1 (Alderson, 2002). After reviewing the information it was found that the comparison between ARRB standard fatigue test results and results from extra-large bending beam apparatus cannot be related, as the bitumen content and lime content were different as well as different mixing method, therefore omitted from this study. The bitumen content has been reduced by the City of Canning due to the economics imposed by extremely large increases in bitumen prices (4.0% to 3.5%), and a reduction in quicklime content (1.5% to 0.8%) due to cracking of early pavements. In addition, originally mixing was undertaken in two passes (quicklime first, followed by bitumen) whereas now all mixing is undertaken in a single pass.

Table 1-1: Composition of the Pavement Sample taken from Nicholson Road. (Alderson, Allan, 2002)

Location	Bitumen Type	Residual Bitumen Content (% by mass)	Quicklime content (%by mass)	Other Additives	Stabilisation depth (mm)
Nicholson Rd	C170	4	0.8	Foaming agent	320

1.3 Significance

WA has a growing road network, currently comprised of over 18,500 km of State roads, 130,000 km of local roads and 35,000 km of roads in national parks and forests. (Main-Roads-WA, 2013). These roads are widely dispersed, covering an area of over 2.5 million km^2.

The fatigue life of foamed bitumen beams has been investigated by many researchers using the standard four-point fatigue apparatus. Standard beams are normally cut to a size of 50 mm × 62 mm × 400 mm before being placed in the device for fatigue testing. This study has a wide-ranging application to the pavements industry, as it investigates the validity of using a new apparatus to test materials where aggregate sizes may be larger than 50mm by using large beams instead of standard beams to allow beams to be tested where stress concentrations resulting from larger pieces of aggregate can be minimised.

1.4 Objectives and Scope

The proposed research programme is to investigate the assumption that the asphalt fatigue equation is valid for bitumen stabilised materials. The method is to use laboratory test data to either validate the current assumption or to provide a result that shows existing equation is not statistically sound utilising extra-large four-point bending beam apparatus. The objectives

of the research are to:

i) Perform a study re-evaluating the asphalt fatigue formula for in-situ foamed bitumen pavements

ii) Provide data that can lead to greater certainty to designers of in-situ foamed bitumen stabilised pavements.

iii) Determine if the fatigue performance of the material is sufficiently consistent given the variable nature of the in-situ pavement materials to practically apply mechanistic design principles.

iv) Examine and report the relative fatigue performance outputs of foamed bitumen stabilised materials in extra-large four-point bending beam apparatus.

1.5 Thesis outline

The thesis report includes the following Chapters:

- Chapter one, Introduction – objectives and scope of the research.
- Chapter two, Literature review – a review of previous works, including the identification of research gaps.
- Chapter three, Sample preparation – Including; sample source and details of testing conducted on the samples.
- Chapter four, Testing program and equipment – Including an overview of four-point fatigue test, large beam fatigue test apparatus, preliminary testing and a definition of validity.
- Chapter five, Test results and analysis – Including; fatigue life determination, curve fitting, using extrapolation on fatigue results, phase angle and Hysteresis loop studies and Austroads fatigue formula evaluation.
- Chapter six, Summary, Conclusion and recommendation – a summary of findings and conclusion is presented and some recommendations for further research is included in this chapter.

2. LITERATURE REVIEW

2.1 Introduction

A review of the literature relevant to asphalt fatigue life prediction and performance of In-situ foamed bitumen stabilised pavements in Australia and worldwide has been undertaken. The study considered the history and methods of design adopted during the past use of stabilised material and outlined the impacts of the result on the whole of life costs resulting from the application of this technology. Two distinct methods of study applied to the project, the first an experimental study to provide data by undertaking fatigue tests and the second consisting of a numerical investigation to identify the accuracy of the Austroads asphalt fatigue equation to provide data with which to verify and support the claims made in this study. The scope of work presented in this chapter is outlined in Figure 2-1.

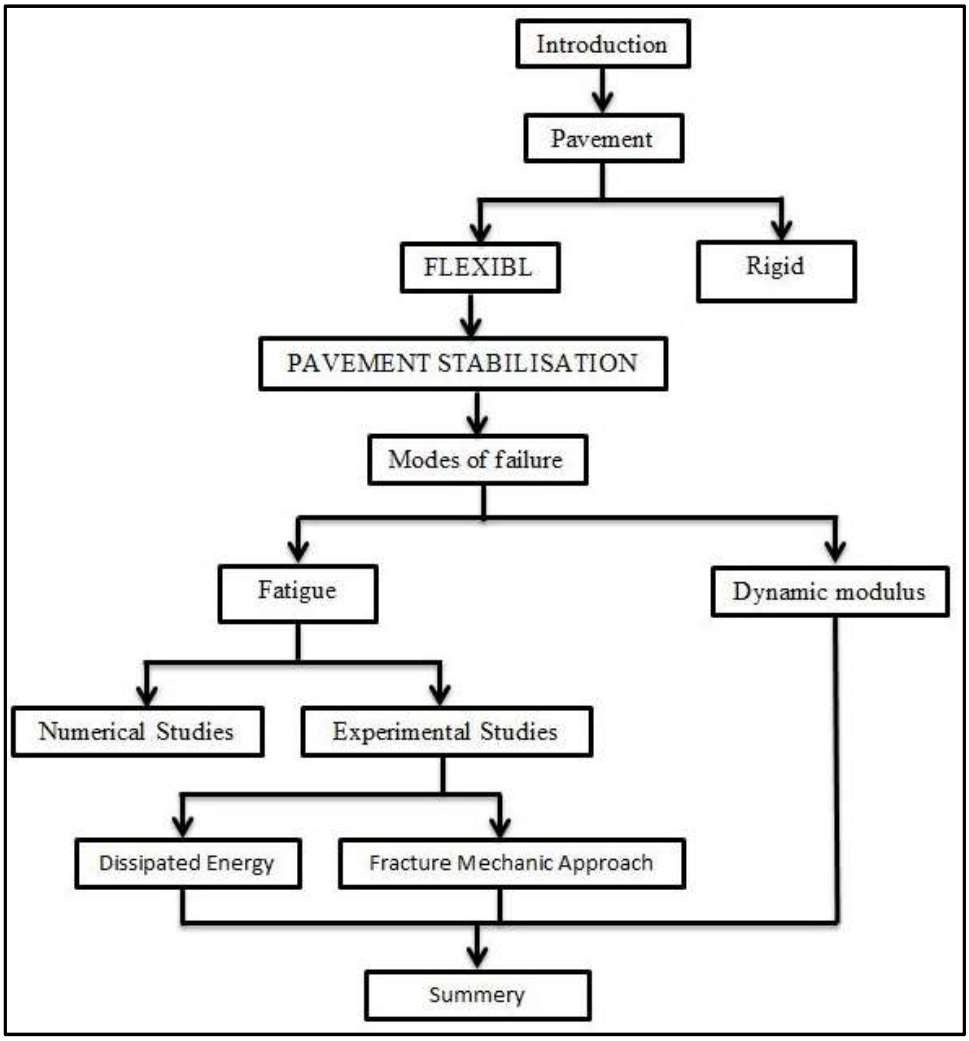

Figure 2-1: Scope of work for Literature review

The results of previous experimental works were examined and compared to the data

obtained during that research.

In asphalt and bound pavements, fatigue cracking occurs when repeated traffic loads induce tensile strains at the base of the bound layers, and eventually after a number of repetitions of strain, cracking initiates at the base of the layer. The properties of the material determine the relationship between the magnitude of strain and the number of repetitions that can be tolerated before cracking commences. This section presents a review of the literature relevant to the fatigue of stabilised pavements and is principally concerned with Western Australian practices and procedures.

The methods used to stabilised flexible pavements are also discussed in this section with the main focus being on the in-situ foamed bitumen stabilisation method.

The City of Canning in Western Australia commenced using the foamed bitumen stabilisation process in 1999 but recognised the limitations in available knowledge to confidently design the stabilised pavements. The City engaged ARRB Transport Research (ARRB TR) to undertake fatigue testing and research into samples taken from completed roads. (Leek, 2002)

Testing involved four-point fatigue beam testing and was reported by Alderson (2000a, 2000b & 2000c) which sought to make general conclusions about the stabilisation process and the relative laboratory fatigue performance of the materials studied. Samples from these sites were tested in the laboratory using a four-point bending beam test in controlled strain mode to determine the fatigue performance.

Australian Road Research Board of Transport Research (ARRB TR) documented additional studies to answer some of the questions raised by an extensive investigation into the performance of foamed bitumen/lime materials stabilised in-situ. The studies included experimental work undertaken at the ARRB TR laboratories and a review of the literature to answer some fundamental questions dealing with pavement performance models (Alderson, 2001). An additional study which involved five sites from four pavements in the City of Canning was again undertaken by ARRB TR (Alderson, 2002)

In 2008, two sections of pavement were selected for a repeat round of fatigue tests, and three sections for repeat Indirect Tensile Modulus Testing. The fatigue testing was undertaken by ARRB TR and the Indirect Tensile Modulus Testing by ASLAB.

The results of the repeat testing indicate that the flexural modulus may have increased marginally over the nine-year period, and this is considered a reliable result. There appears also to have been an increase in remaining fatigue life, but given the variability of the fatigue part of the test, the variation may not be significant (Leek, 2013).

2.2 Pavement

A pavement is a combination of several layers of suitable material constructed over the in-situ soil, called the subgrade, and is designed to transfer the vehicle load to the subgrade at a vertical compressive strain that can be tolerated by the particular subgrade material.

Pavements are classified as either flexible (containing unbound granular and/or stabilised materials and/or asphalt), rigid (concrete pavement with joints and/or steel reinforcement) or composite pavements (Austroads, 2005).

As the focus of this study is on foam bitumen stabilised pavements that fall into the flexible category, rigid pavements will not be considered in this review. In most of the flexible pavements, the wearing course is asphalt, all other layers are granular. The major components of flexible pavements are shown in Figure 2-2. A capping layer is only for very weak subgrades and not a common practice in Australia.

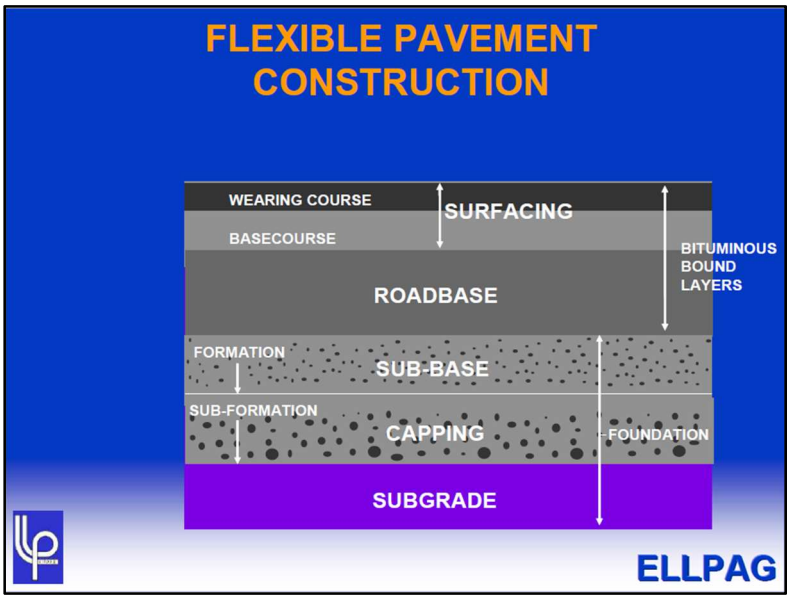

Figure 2-2: Flexible pavement construction (ELLPAG, 2006)

Under traffic load, the behaviour of a flexible pavement with bound layers is shown in Figure 2-3**.** Due to deformation of pavement, the horizontal tensile strain is induced at the base of bound layers only, and vertical compressive strain induced at the top of all layers and

the subgrade.

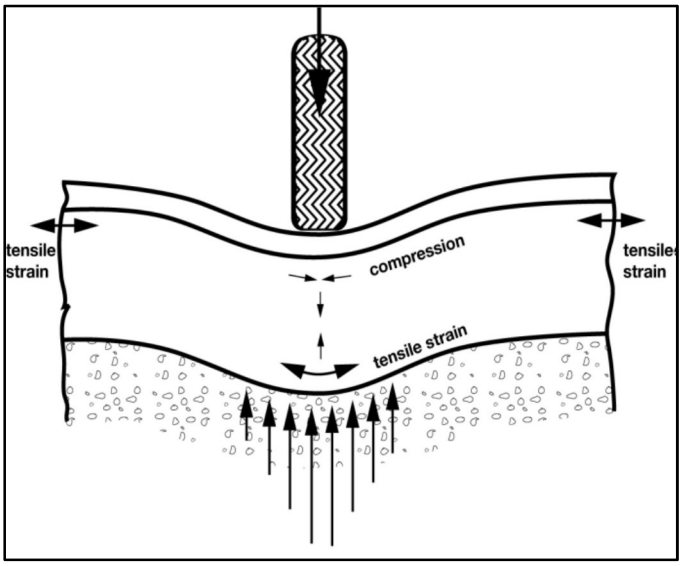

Figure 2-3: Response of flexible pavement to load (Austroads, 2005)

Rigid pavements under traffic load distribute strain on subgrade in a more uniform way as per Figure 2-4.

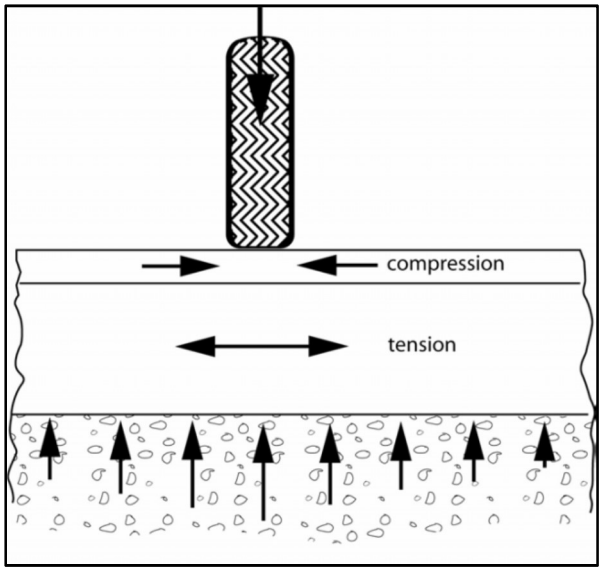

Figure 2-4: Response of rigid pavement to load (Austroads, 2005)

2.3 Flexible Pavement

Almost 98% of Australian road networks are paved with the flexible pavement, composed of a granular base course and bitumen surfacing. (ARRB, 2013)

The base and subbase layers in flexible pavement provide most of the structural capacity in terms of load spreading ability within the pavement (Austroads, 2005). In the case of

structural asphalt, the middle structural layers carry most of the load, as distinct from the wearing course.

According to Austroads Guide to Pavement Technology Part 4A, (Austroads, 2008), the functions of a granular base layer in a pavement are to:

- Provide sufficient stiffness to support the surfacing layers.
- Provide sufficient stiffness to distribute loads to the subgrade or subbase
- Provide high durability to withstand surface contact stresses.
- Provide a layer with minimal deformation under repeated loading.
- Provide a low permeable layer.

However a correctly designed granular pavement has a finite life, and this life may be reduced as changed in traffic demographics occur over time; heavier legal load limits, deregulation of transport and traffic growth with the demands of a growing population may mean that the pavement is no longer structurally capable of supporting current traffic at the time rehabilitation is required. When an existing pavement is subjected to a major treatment that increases its level of service, it is said to be rehabilitated.

As previously mentioned, granular pavements have been designed using empirical design charts commonly referred to as Austroads Figure 8.4. It is not often understood that this design chart whilst providing the required cover over the subgrade, does not predict the fatigue life of the asphalt surface, this is controlled largely by the quality of the base layer.

2.4 Pavement Rehabilitation

The rehabilitation of a granular pavement is mainly undertaken to correct distress issues such as fatigue cracking, rutting, subsidence, depressions and other distress items which affect surface level. On occasions, some distress may initiate through environmental cracking allowing moisture to penetrate and weaken the base layers.

There are many factors need to be taken into account to determine rehabilitation solutions other than structural consideration: the safety of workers and road users, effect of works on existing traffic, effect of road rehabilitation on local business profits, adjacent roadside furniture such as kerbs, driveways, medians and paths, etc., existing pavement thickness, traffic volumes and types, existing pavement materials, future maintenance access, the cost of

construction, varying life of treatments.

Where heavy traffic conditions apply, such as on major truck routes, rehabilitation by granular overlays and thin asphalt has often resulted in early asphalt fatigue failure, as the granular base material takes some years to reach ultimate stiffness.

The main pavement rehabilitation methods include asphalt and granular overlays, mill and overlay with deeper strength asphalt, and in-situ recycling options including cold in-place recycling, and in situ stabilisation with chemicals, cement, pozzolanic materials and bitumen both emulsion and foamed.

Each option has its own strengths and weaknesses. Choosing the rehabilitation option should be done by taking into account design and construction considerations including; road geometry, drainage considerations, safety, and structural considerations. However, issues related to timing and funding, traffic management, road user costs, effects on business operations and future maintenance (the whole of life costs) must be applied. (Queensland Department of Transport and Main Roads Pavements, 2012). In more recent times, issues associated with sustainability including both resource conservation and energy consumption need to be considered.

These were some of the factors facing the City of Canning when faced with the rehabilitation of existing heavily trafficked roads, which were generally poorly designed for the traffic loading at the time of construction, and changes in traffic volumes and increased axle loads meant that simple resurfacing was not a viable solution. When faced with the rehabilitation of a High Road near a major shopping centre in 1999, and Nicholson Road, a major commuter and heavy transport route in 1999, there were several options available (Leek, 2002):

The first option was a full reconstruction by removal of the existing pavement, removal of subgrade material and replacement of thicker pavements at the existing levels. This option was discounted for several major reasons; the cost was prohibitive to the City, the cost of delays to traffic and businesses for the very long periods of construction was considered unacceptable, and required the closure of one carriageway, and every day, the risks to other road users were exacerbated and the road could not be opened at night.

The second option was a granular overlay of the existing pavements requiring alterations to drainage, driveways and medians. This option was discounted for following major reasons; the cost was prohibitive, it required a 150mm raising of the pavement to achieve the required thickness, resulting in major disruption to access and drainage of adjacent properties, and while less time consuming than full reconstruction, it was still an unacceptably long construction period and while the road could be opened at night, the loose material and dust would provide a temporary hazardous surface

The third option discussed as replacement of the existing pavement with full depth asphalt. This option also was discounted as; it was very costly, it required removal of large depths of the existing pavement resulting in logistical difficulties, whilst construction periods were lesser than the granular options; it was a longer period than the fourth option, insitu stabilisation.

The fourth option, adoption of a new process not undertaken previously in Western Australia, in-situ foamed bitumen stabilisation this option was chosen as it was the cheapest option, it was the fastest construction process, there was no issue with levels as no excavations were required, and provided a safe, dust free temporary surface overnight.

With the successful implementation of the rehabilitation of those, and two other roads in 1999 using the in-situ foamed bitumen stabilisation, this method became the method of choice for the City of Canning in the rehabilitation of heavy-duty pavements.

In these initial projects, the fatigue life of the pavement was predicted using the asphalt fatigue equation, however, in his paper, (Leek, 2002) stated:

> *"In the design process, it was assumed that the flexural modulus of the stabilised layer would be 2400 MPa, and that the fatigue life of the stabilised material would be equivalent to asphalt. Whilst there was some confidence in the assumed modulus value based on the initial Mobil laboratory test results, the assumption that the asphalt fatigue equation could be used with confidence was considered questionable. Asphalt is a manufactured product made to close grading tolerances, and it was considered that the fatigue life of an in-situ stabilised material could be quite variable due to grading differences".*
>
> *"Also, the most often reported modulus value for a stabilised material is the indirect*

tensile modulus as determined in the MATTA device, rather than the flexural modulus required in the mechanistic design process".

Furthermore, in the recommendations, (Leek, 2002) stated:

> *"The testing undertaken indicates that there is considerable variation in fatigue performance within the material and that the recommended design model of using the asphalt fatigue equation may not valid. Further research to validate this conclusion and to determine the existence of a unique equation is required".*

Currently, except the City of Canning, in Australia the fatigue life of, in-situ foamed bitumen stabilised materials continues to be estimated using the Austroads asphalt equation.

2.5 Pavement Stabilisation

In the case of the unavailability of or cost to provide suitable high-quality base course materials, stabilisation methods can be used to satisfy the characteristic needs such as strength and stability for low-quality granular material. In the case of an unbound granular pavement which has reached the end of its structural life, or changes in traffic demographics have resulted in the pavement structure no longer being sufficient, stabilisation can be applied to restore the pavement function due to higher material performance characteristics.

Stabilisation is a process to alter the properties of a pavement material, generally by adding a stabilising agent to improve operating performance (Austroads, 2006). There are different types of additives and design procedures available for base stabilisation. Some of these include modified materials using lime, pozzolans or cement, foamed or emulsified bitumen as well as dry powder polymers which are ideal for treating natural gravel especially moisture sensitive gravels (AustStab, 2007), but rely on the material having a reasonable clay content. The selection of the binder may be affected by the geological history of the pavement material or the local climatic conditions.

2.6 Foamed Bitumen stabilisation

Foamed bitumen stabilised material refers to those materials where the stabilisation method is of hot bitumen, foamed using air and water, and mixed into the existing pavement material.

Instantaneous expansion of the bitumen will result when a small quantity of water is injected

into hot bitumen, causing an approximate 15 times expansion of its original volume. The large surface area of the foamed bitumen's helps it to mix with the existing pavement material in the mixing chamber of the stabiliser (Austroads, 2006).

The procedure of production of foamed bitumen is illustrated in Figure 2-5.

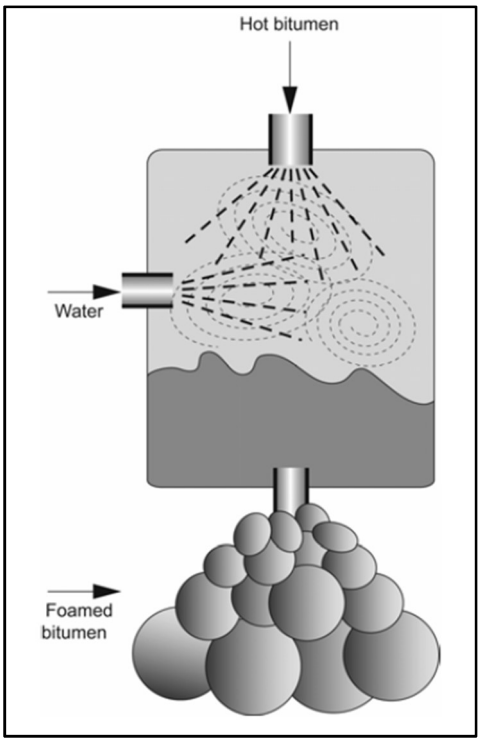

Figure 2-5: Manufacture of foamed bitumen. (Austroads, 2006)

2.6.1 Characterisation of foamed bitumen

Foamed bitumen or expanded bitumen is produced by temporarily converting the bitumen from a liquid to a foam state using heat and by the addition of a small percentage of water. (Muthen, 1998)

In terms of characterisation, the foamed bitumen is categorised by two main properties; Expansion Ratio (ER) which is the ratio between maximum foam state volume and the volume of bitumen after the foam has completely dissipated and Half-Life (HL) defined as time that takes foam bitumen collapse to its half size volume (Sunarjono, 2013). Generally to produce a higher quality foamed bitumen a higher expansion ratio and half-life is required (Huan, 2014). Figure 2-6: ER and HL relationship (after Austroads, 2011) gives an example of how to determine these properties.

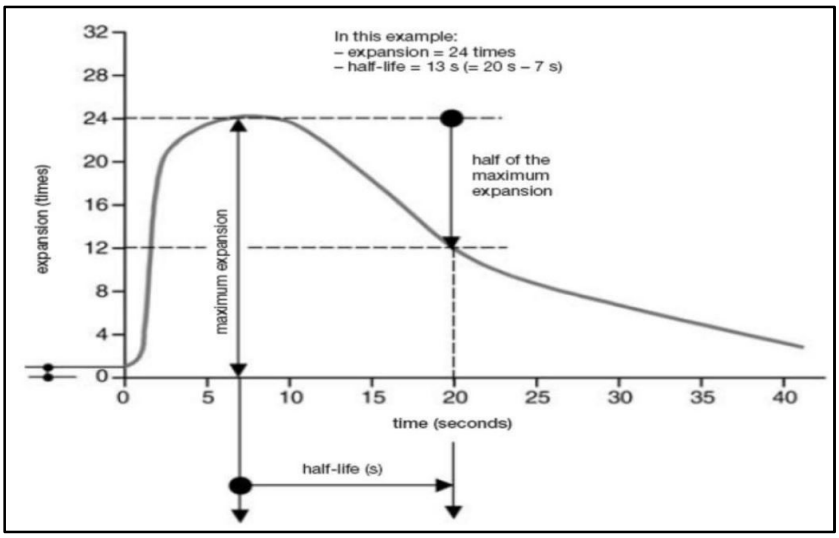

Figure 2-6: ER and HL relationship (after Austroads, 2011)

Foaming Water Content (FWC) is the amount of water (by bitumen mass) added to bitumen during the foaming process. FWC can affect both ER and HL significantly. (Jenkins, et al., 1999)

Tensile Stiffness Modulus (TSM) of foamed bitumen asphalt also is affected by FWC. The optimum TSM is achieved at FWC equal to 5 % (Sunarjono, 2013)

2.6.2 Foamed Bitumen Stabilised material Properties

Foamed Bitumen Stabilised (FBS) is a material with unique properties. (FBS) is a flexible viscoelastic medium which is strong and water resistant. A suitable (FBS) has bitumen content of typically 3.0% by weight with 1% to1.5% amounts of active filler by weight (Browne, 2015). However, other researchers considered a range between 2.5% to 4% as suitable FBS. The range is dependent on the design philosophy and material properties. The preferred bitumen for foamed bitumen is class 170 bitumen (Ramanujam & Jones, 2000).

2.7 Benefits of using stabilised material

There are many advantages such as the social, environmental and economic benefits in utilising stabilisation in pavement rehabilitation. Social benefits include faster project completion time, less user impact, improved road safety and pollution reduction. Environmental benefits include reduced raw material demand, reduced energy requirements (Austroads, 1998) and recycling reduce industrial waste and landfill (Wilmot & Vorobieff, 1997) assisting with the Government Sustainability Agenda (White, 2006). Economic benefits are direct costs such as the improved whole of life costs and reduced upfront costs,

and indirect costs such as minimising traffic delays and business losses. (Wilmot, 1991).

2.8 Modes of failure of flexible pavements

There are many often interrelated causes for the deterioration of flexible pavements. Under repeated load over a period of time, the magnitude of stress and strain generated in the pavement failure is associated with the rate and magnitude of the failure mode. (Adlinge & Gupta, 2013).

Asphalt pavement surface distresses are categorised into four major groups. (Adlinge & Gupta, 2013)

- The first group is cracking that includes:
  - Fatigue cracking(Alligator cracking), caused by excessive flexure
  - Longitudinal cracking, caused by subgrade volume changes, trenches
  - Transverse cracking caused by some of the same causes as longitudinal cracks, but may also result from cementing and shrinkage of base layers
  - Block cracking, caused by intersecting transverse and longitudinal cracks resulting from cementing and shrinkage of base layers
  - Slippage cracking, caused by the horizontal forces from traffic
  - Reflective cracking caused after overlaying pavement that cracks from lower layer will reflect new surface.
  - Edge cracking, caused by lack of support of the shoulder due to weak material or moisture
- The second group is surface deformation including:
  - Rutting resulting from densification of pavement layers or subgrade
  - Corrugations resulting from low cohesion of granular layers,
  - Shoving resulting from shear failure of pavement layers or subgrade,
  - Depressions resulting from subsidence, poor compaction or decay of organic materials,
  - Swell resulting from volume changes from expansive soils.
- The third group is disintegration,
  - potholes resulting from high pore pressures developing when vehicles induce load into saturated pavement materials
  - stripping resulting from a lack of adhesion between bitumen and aggregate

- The last group is surface defects that include:
  - Ravelling resulting from oxidation of the bitumen in aged asphalts or spray seals,
  - Bleeding resulting from excess bitumen in asphalt or spray seals,
  - Polishing resulting from poor aggregate selection and
  - Delamination resulting from a poor bond between successive pavement layers.

Fatigue cracking in an asphalt surface results from greater than expected traffic loading, or poor base material performance, and may be associated with rutting and shoving. It is these structural type failures that in situ foamed bitumen stabilisation is particularly useful in addressing.

However if fatigue is itself a mode of failure associated with foamed bitumen, then the industry needs to be confident that the assumptions made in the thickness design of the stabilised layer are sound.

2.9 Fatigue and dynamic modulus in foamed bitumen stabilised material

2.9.1 Fatigue

Fatigue cracking, as one of the most common pavement failure modes, exhibits as a series of interconnected cracks at the surface of stabilised material (or HMA) and is associated with the strain induced by repetitive traffic loads. Fatigue cracking could initiate at top or bottom of pavement. (Asadi et al. 2013; Pavement Interactive 2007)

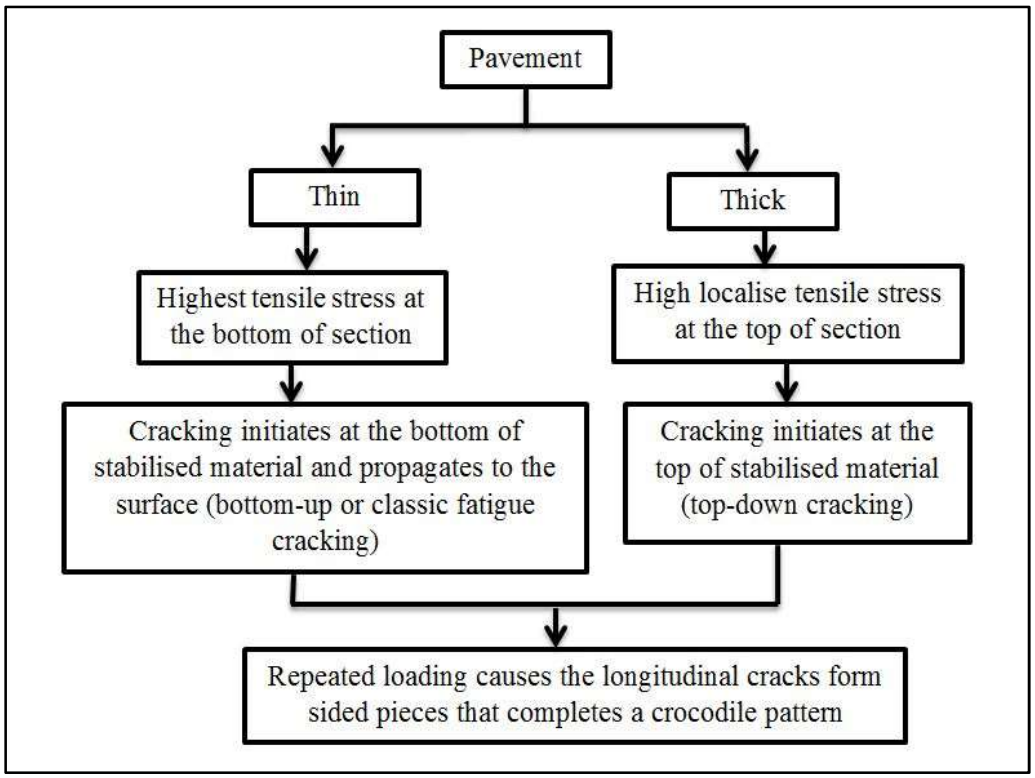

Figure 2-7: Fatigue cracking description

To enable the design of a bound pavement it is essential to understand the performance of the bound layer. In order to obtain this data traditionally requires many laboratory tests under different loads, load time, rest period and environmental conditions (Baburamani, 1999).

Different parameters affect the fatigue performance of a thin asphalt on a granular base and a flexible pavement containing thick asphalt or foamed bitumen stabilised material. In the asphalt pavements on a granular base, the structural capacity is determined by the base modulus, and the asphalt must be flexible and fatigue resistant under heavy traffic due to the high deflections under load. In this state, high stiffness is a disadvantage. In deep strength asphalt pavements and foamed bitumen, the bound material takes the major load spreading function. Here high modulus limits strain and hence fatigue. (Leek, 2013)

2.9.2 Numerical Investigations

There were few studies that were identified which investigated the fatigue behaviour of pavement slabs using numerical finite element (FE) analysis.

Buttlar et al. (2006) provided a theoretical formulation for the graded finite element method by using the user material subroutine UMAT capability of the finite element software ABAQUS.

Aure and Ioannides (2012) studied fatigue behaviour of pavement slabs using (FE) analysis. The FE program ABAQUS was used in the study. The influence of softening curve, cohesive zone width and mesh, loading mode, tensile strength, and fracture energy was also examined.

It was concluded that the calculated stresses in the mastic mechanism are in line with the computed strength values, meaning 2D models were very consistent to determine stress states in the mastic of the asphalt mix.

As the focus of this study is in experimental studies, numerical studies will not be discussed further in this study.

2.9.3 Experimental Investigations

Two methods have been suggested in the literature to investigate the laboratory fatigue behaviour of foamed bitumen stabilised pavement. The main approaches can be categorised as strain-stress approach and dissipated energy approach.

During the period 2008–2011, NZ Transport Agency conducted flexural beam breakage and fatigue tests on large beams that were compacted in rectangular moulds 530mm long by 150mm square. The apparatus used is shown in Figure 2-8

Figure 2-8 : Modified RLT Testing equipment (NZ Transport Agency 2012)

2.9.4 Strain-stress approach

The fatigue life of pavement materials is defined as the number of cycles, N_f, at which the stiffness will be reduced to 50% of initial stiffness. (Artamendi & Khalid, 2013). During past half-centennial different researchers have proposed models to predict pavement fatigue life.

First, rational pavement design conceived during the 1960s by Dorman 1962, Pell (1962) and Monismith et al. (1961). Their simple and well-known fatigue life prediction models relate the tensile stress or strain to the fatigue life using experimental coefficients as shown in 2-1 and 2-2.

$$N_f = K_1 \left(\frac{1}{\varepsilon_t}\right)^{k_2} \quad \text{2-1}$$

$$N_f = K_1 \left(\frac{1}{\sigma_t}\right)^{k_2} \quad \text{2-2}$$

Where

N_f = fatigue life (cycles)

ε_t = horizontal tensile strain at the bottom of the specimen

σ_t = horizontal tensile stress at the bottom of the specimen

K_1 and K_2 = experimental coefficients obtained from laboratory testing

The initial stiffness of pavement considered as a major parameter in predicting fatigue life by Shell (Shell, 1978) and Asphalt Institue (1982) that led to a modified version of Equation 2-1. The air void content of the mix also has been taken into the account by some researchers who found that air voids and the fatigue life were related (e.g. Pell et al. 1975; Harvey et al. 1995)

The upgraded version of this design method is known as Mechanistic-Empirical (M-E) pavement design, (Das, 2008). The M-E method is widely being used in many countries; Austroads 2004, French 1997, IRC:37 2001, MS-1 1999, NCHRP 2005, Theyse et al. 1996, Shell 1978 and AASHTO 2008 have adopted the M-E pavement design approach.

AASHTO (2008)(Mechanistic-Empirical Pavement Design Guide (MEPDG) adopted this model by suggesting 2-3.

$$N_f = 0.00432 \times K \times C(\varepsilon_t)^{-3.9492} \times (E_1)^{-1.281} \qquad 2\text{-}3$$

Where

N_f = fatigue life (cycles)

ε_t = horizontal tensile strain at the bottom of the specimen

C = 10^M

M = $4.84(\frac{V_{be}}{V_{be}+V_a} - 0.69)$

K = $$\frac{1}{0.000398 + \frac{0.003602}{1 + e^{(11.02-3.49h_{ac})}}}$$

V_{be} = effective binder content (%)

V_a = air void content (%)

The fatigue life of asphalt in Australia is predicting using asphalt fatigue transfer function (FTF) as applied in the Austroads Guide to Pavement Technology Part 2, Structural Design, this being as Equation 1-1 and presented in chapter one of this thesis. However it is again noted that the Shell method (Shell 1978) assumes an isotropic subgrade and notes a shift factor of 10 or more is applicable to convert to field use, Austroads uses the same equation but applies anisotropic properties and no shift factor.

2.9.4.1 Derivation of shell fatigue transfer function

The Shell FTF derived from the fatigue data provided by Van Dijk and Visser (Van Dijk & Visser, 1997) from their work that was carried out on 13 asphalt and base course mixtures listed in Table 2-1

Mix Type	Binder Grade	Binder Volume (%)	Air Voids (%)	Voids in mineral aggregate VMA (%)
Asphalt Concrete State of California	40/50	14.2	1.7	15.9
Dense Asphaltic Concrete	40/50	11.4	1.9	13.3
Gravel Bitumen French	40/50	9.3	9.3	18.6
Dense Bitumen Macadam	40/60	11	3.6	14.6
Rolled Asphalt Base Course Mix	40/60	14.1	2.2	16.3
Bitumen Sand Base Course	45/60	8.9	20.3	29.2
Gravel Sand Asphalt, Dutch (Stroe)	45/60	11	11	22
Rich Sand Sheet	45/60	19.3	7.8	27.1
Gravel; Sand Asphalt Dutch (Muiden)	50/60	13.3	6.6	19.9
Dense Bitumen Macadam	80/100	11	3.4	14.4
Lean Bitumen Macadam	80/100	4.9	33.2	38.1
Lean Sand Asphalt	80/100	10.5	8.4	18.9
Asphalt Base Course Mix German (Struttgart)	B80	9.3	2.6	11.9

Table 2-1: Composition of asphalt mixes used in the development of the Shell life prediction model (Claessen, et al. 1977).

These mixes were asphalts from various countries including France, Netherlands, America, England and Germany. They are not foamed bitumen asphalt and not from Australia.

Two assumptions were used in the derivation of the Shell FTF. Firstly the exponent in the FTF, which is $N_f = kx{\varepsilon_{fat}}^{-n} = 5$, is assumed to be equal to five (n=5) for all of the asphalt mixes. This exponent normally varied between 4–6 (Van Dijk & Visser, 1997).

It was also assumed that the slopes of the $\log \varepsilon_t$ versus $\log S_{mix}$ is equal to 0.36 (Stubbs, 2011).

The reliability factor (RF) in Equation 1-1 is a transfer function that relates laboratory fatigue life to the in-service fatigue life. RF takes into account the differences between laboratory and in-service conditions also variability from construction, environment, and traffic loading. (Stubbs, 2011) However, it remains significantly more conservative than the Shell model.

2.9.5 Dissipated energy approach

Fatigue failure based on dissipated energy has been defined as energy ratio that the number of cycles, N1, where microcracks occur. Energy ratio is equal to dissipated energy at cycle N divided by cumulative dissipated energy up to n-cycle as per Equation 2-4.

$$R_n = \frac{\pi \sum_{i=0}^{n} \sigma_i \varepsilon_i \sin \emptyset_i}{\pi \sigma_n \varepsilon_n \sin \emptyset_n} \quad 2\text{-}4$$

Where

σ = stress

ε = strain

$\emptyset$ = phase angle

Van et al. (1972) proposed a model that relates the fatigue life of asphalt mixes to cumulative dissipated energy as in Equation 2-5.

$$W_{fatigue} = AN_f^Z \quad 2\text{-}5$$

Where

$W_{fatigue}$ = cumulative dissipated energy when fatigue failure occurs

N_f = number of cycles to fatigue failure

A & Z = experimental coefficient obtainable from laboratory test data

Hopman et al. (1989), Pronk and Hopman (1990), Rowe (1993), Carpenter and Jansen (1997), Rowe and Bouldin (2000) and Abojaradeh (2003) used the energy ratio approach to predict the fatigue life of asphalt. (Souliman, 2012)

2.9.5.1 RDEC Approach (ratio of dissipated energy change)

A model independent of the testing conditions and based on the fatigue-healing model was developed by Carpenter and Shen (Shen & Carpenter, 2007), and Shen et al. (2010), Moghadas Nejad, Notash and Forough (Nejad, et al., 2015) Shen et al. (2010) cited

"... not all DE is responsible for fatigue damage, only the relative amount of energy dissipation coming from each additional load cycle, while excluding the energy dissipated through passive behaviours such as plastic DE, viscoelastic damping, and thermal energy, will produce further damage."

The relationship between the dissipated energy ratio change for the cyclic displacement/strain-controlled tests from cycles m to n and the energy after cycles m and n is shown in Equation 2-6.

$$RDEC_n = \frac{(DE_m - DE_n)}{DE_m(n-m)} \quad 2\text{-}6$$

Where

$RDEC_n$ = dissipated energy ratio change from cycle m to n

DE_m = dissipated energy at cycle m

DE_n = dissipated energy at cycle n

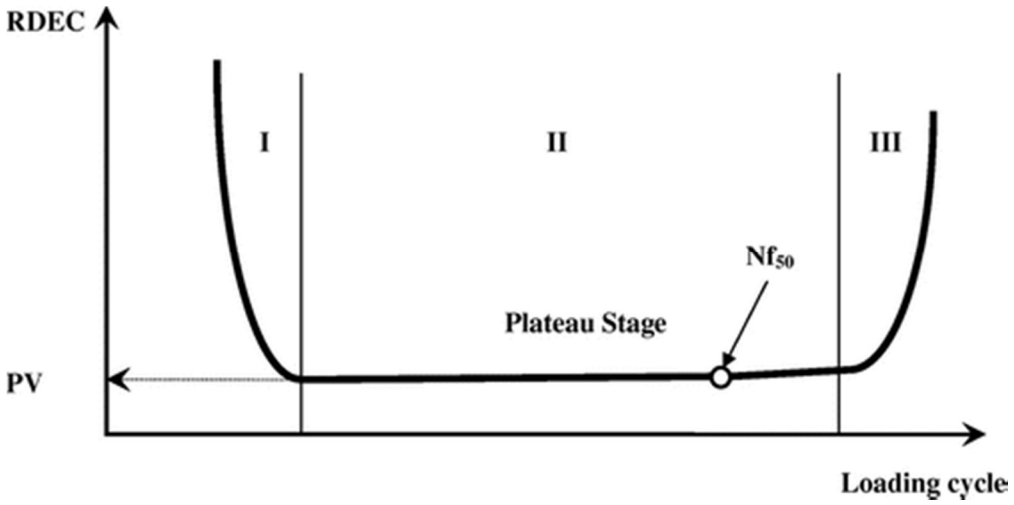

Figure 2-9: RDEC versus loading-cycle curve having three distinct stages ((Nejad, et al., 2015)

By plotting RDEC values verse as loading cycles as shown in Figure 2-9, three separate stages may be obtained: stage I, RDEC will rapidly decrease during the initial loading cycles, stage II, in which the RDEC is flat, and stage III with an increase in RDEC values until fatigue failure. (Nejad, et al., 2015)

The plateau stage is the period where input energy is converted into damage. The plateau value (PV) is the RDEC value corresponding to the loading cycle with 50% reduction in the initial stiffness (Shen & Carpenter, 2007). Fatigue failure will occur at the Plateau stage.

2.10 Pavement functionality under the real parameters.

Figure 2-10 shows an illustrating diagram of effective inputs into the fatigue equation (Priest & Timm, 2006). Environmental and traffic factors are two important factors that require a huge amount of samples to consider different weather conditions and different types of traffic.

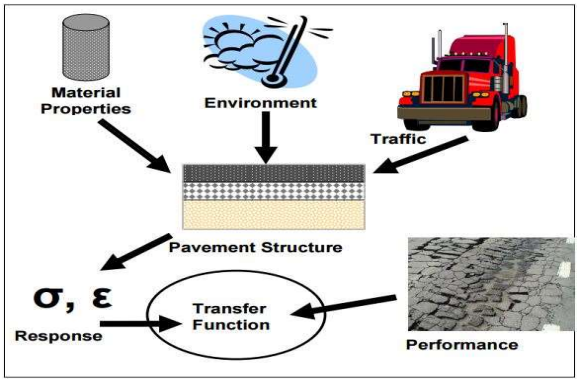

Figure 2-10: Illustration of Transfer Function Development. (Priest & Timm, 2006)

2.11 Summary

The study considered the history and methods of design adopted during the past use of asphalt mix and stabilised material.

The different approaches can be summarised as follows:

- experimental approach
  - strain-stress approach (phenomenological approach)
  - dissipated energy approach

The four-point fatigue test has been described as the time-consuming procedure by almost all of researchers. (Bocz, 2009)

2.11.1 Study gaps

All of the fatigue testing programs reported were conducted on standard asphalt sized beams, where there are significant concerns due to the scale of the aggregate to beam size.

There are few studies that were identified which were relevant to typical foamed stabilised material used in Western Australia.

Only one other New Zealand study was identified where non-standard large beams in rectangular moulds (530mm long, 150mm wide and 150mm thick) were tested, however, this was not a foam bitumen stabilised material fatigue based test.

As the work reported in this thesis involves conducting four-point fatigue test on large beams in a temperature controlled cabin, for the first time it will help to investigate the suitability of using AGPT02 (Austroads, 2012) asphalt fatigue equation for foamed bitumen stabilised materials.

3. SAMPLE PREPARATION

3.1 Sample source

For the experimental component of the research 14 samples were taken from slabs previously cut from roads within the City of Canning. These samples were considered useful, as they were composed of the same materials types that had been previously tested by ARRB Transport Research for the City of Canning.

The large beams were cut from 2 different slabs, one slab from Kewdale Road and one slab from Nicholson Road where the composition of the mix was made up of asphalt, granite road base and limestone. Figure 3-1 shows the slabs of the pavement material that were made available for testing.

Figure 3-1: Large beams stored after the first cut from slabs.

The beams were cut to size using the circular saw located at the Geomechanics Laboratory at Curtin University as shown in Figure 3-2 to produce beams ready for testing as shown in Figure 3-2 and Figure 3-3.

Figure 3-2: Large beams during a final cut in Curtin laboratory

Figure 3-3: Large beams after a cut in Curtin laboratory.

3.2 Details of testing conducted on the samples

Laboratory testing including particle size distribution (PSD), Bulk Density, Air-void, Maximum Density, Binder Content tests were undertaken to determine the physical characteristics of the base materials.

3.2.1 Determination of binder content

The Centrifuge extractor machines as shown in Figure 3-4 and Figure 3-5 located in the Geomechanics laboratory was used to extract the bitumen from the core material after crushing and the addition of solvent. The material was preheated in ovens able to maintain a temperature of 105°C to 110°C. The solvents required for the extraction, mineral turpentine and toluene were obtained from marked containers held at the laboratory.

Figure 3-4: Centrifuge Extractor in Curtin laboratory.

Figure 3-5: Centrifuge machine in Curtin laboratory.

Following solvents, shown in Figure 3-6, were used to extract the bitumen from the aggregate:

- Mineral turpentine
- Toluene

Figure 3-6: Solvents used for asphalt extraction test.

However it is important to note that the original pavement was composed of some asphalt (approximately 10%) and the bitumen in these materials is not mobilised in the stabilisation process, but cannot be separated in the extraction process.

Two beams were selected, one from each pavement slab. The samples were gently warmed and split into two representative portions and a binder content determination performed in accordance with MRWA 730.1 – Bitumen content and particle size distribution of asphalt and stabilised soil: Centrifuge method.

$$Bit = \frac{m_1 - [(m_5 - m_4) + m_{FR} + m_{EF}]}{m_1} \times 100 \qquad 3\text{-}1$$

Where

m_1 = mass of test portion in grammes

Bit = bitumen content as a percentage

m_4 = mass of oven dish in grammes

m_5 = mass of the oven dish and contents in grammes

m_{FR} = mass of matter on the filter ring in grammes

m_{EF} = mass of matter in extraction fluid in grammes

The binder content results are shown in Table 3-1.

Table 3-1: Bitumen Contents of Samples

Sample number	Bitumen Contents (%by mass)	Bitumen Contents (%by volume)
8	1.80	4.1
11	3.12	6.6

To explain the volumetric properties of asphalt mix, asphalt phase diagram is presented in Figure 3-7.

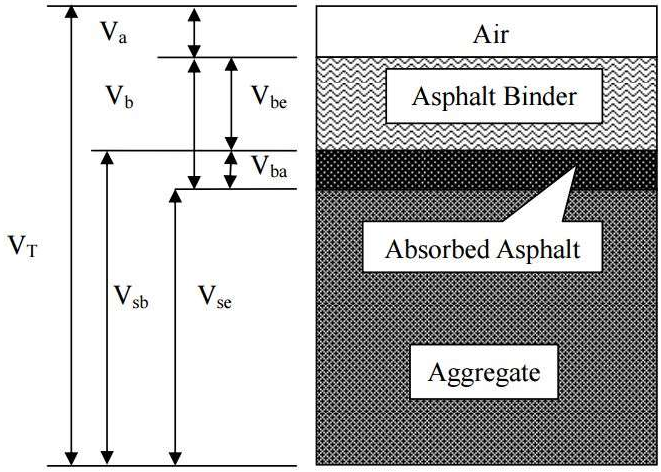

Figure 3-7: Three phase diagram for an Asphalt mixture (YU, 2012)

Where

V_a = Volume of Air

V_b = Volume of Bitumen

V_{be} = Effective binder volume

V_{ba} = Absorbed binder volume

V_{sb} = Bulk aggregate volume

V_{se} = Effective aggregate volume

V_T = Total volume

3.2.2 Particle Size Distribution

Following the removal of bitumen from the aggregates, a particle size distribution was performed in accordance with WA 730.1 – Bitumen content and particle size distribution of asphalt and stabilised soil: Centrifuge method. The results are shown in Table 3-2 and Figure 3-8.

Table 3-2: Particle Size Distribution

Sieve size (mm)	19	13.2	9.5	6.7	4.75	2.36	1.18	0.6	0.3	0.15	0.075
Percentage Passing for Sample 8	100	96	89	80	70	53	42	32	20	11	6.9
Percentage Passing for Sample 11	100	94	80	71	62	49	37	28	17	9	4.3

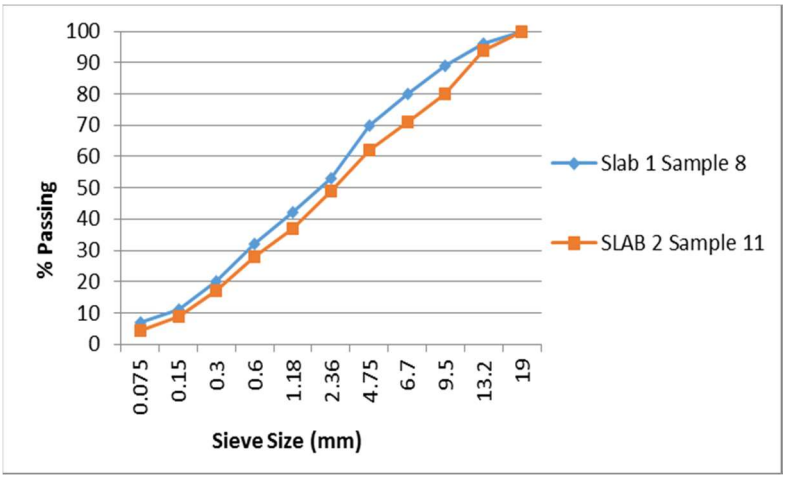

Figure 3-8: Aggregate mix PSD

3.2.3 Bulk density

The mass of the beams was determined before testing to determine mensuration bulk density of the beams, also cores have been taken from beams after fatigue testing and this allowed Bulk density to be calculated using the pre-saturation method. The bulk density was determined in accordance with AS2891.9.2. The bulk density of 2 slabs is shown in Table 3-3.

$$bd = \frac{(0.997m_1)}{(m_3 - m_2)} \quad \text{3-2}$$

Where

m_1 = Final mass of beam in air

m_2 = Mass of beam in water

m_3 = Mass of beam in air SSD

bd = Bulk density

Table 3-3: bulk density results of foamed bitumen material

Sample number	Bulk density
8	2.062
11	1.935

3.2.4 Air Void

The maximum density of each slab is used to calculate the air voids. The maximum density of slab 1 is 2.07 t/m3 and for slab 2 is 2.03 t/m3.

$$V_a = 100 \times \frac{(G_{mm} - G_{mb})}{G_{mm}} \quad \text{3-3}$$

Where

V_a = % air voids

G_{mm} = maximum density

G_{mb} = bulk density (t/m3)

Table 3-4: Density and air void of the samples.

Sample number	Air void (%)	Maximum density (t/m^3)	Bulk density (t/m^3)
8	4.98	2.17	2.062
11	4.68	2.03	1.935

3.2.5 Standards used

Standards that have been used in sample preparation procedure are listed in the Table 3-5.

Table 3-5: Standards used in regards to sample preparation

Standard	Title	Year
AS 2891.9.2	Determination of bulk density of compacted asphalt – Pre-saturation method	2005
WA 730.1	Bitumen content and particle size distribution of asphalt and stabilised soil: Centrifuge method	2011

Figure 3-9: Determining large beams weight in Curtin laboratory.

Figure 3-9 shows a large beam during weigh in Curtin University laboratory. Cylindered cores, shown in Figure 3-10 were also cut from the large beams after the fatigue test and used to determine the bitumen contents of beams.

Figure 3-10: Core to be used for bitumen content determination

4. TESTING PROGRAM AND EQUIPMENT

4.1 Four-point fatigue test on large beams overview

Fatigue testing is carried out at 20ºC using a large custom made third-point flexural beam apparatus, as shown in Figure 4-1. Specimens previously obtained from Nicholson Road and Kewdale Road measuring approximately 800 x 150 (depth) x 180 mm (width), were subjected to continuous Haversine loading at 10 Hz and at constant strain levels of 150, 200, 400με. Failure was taken as the number of cycles when the flexural stiffness reduced to 50% of the initial value measured at 50 cycles or when 1.5 million cycles were reached. Figure 4-2 shows a sample after failure due to four-point fatigue test.

Table 4-1: Standard used for Fatigue life

Standard	Title	Year
AG:PT/T233	Fatigue life of compacted Bituminous Mixes	2005

(a) **(b)**

Figure 4-1: Large beams during fatigue test, (a) and four-point fatigue test apparatus inside the cabinet, (b) in Curtin laboratory

Figure 4-2: Large beams after four-point fatigue test in Curtin laboratory.

4.2 Large beam fatigue test machine

The EN custom made Tester is a four-point fatigue bending beam apparatus which runs fatigue tests on large beams instead of standard beams cut from slabs (Figure 3-6). The software that used in this study was UTS18. The hardware is also compatible with some of other software developed by IPC Global Company (known as UTS15 and UTS19).

The apparatus was installed in the temperature-controlled cabin. The custom large scale version of the standard IPC Global four-point bending beam apparatus based at the Geomechanics Laboratory at Curtin University was used to perform fatigue tests on the large beams. This fatigue test machine has been designed by IPC Global under Curtin specifications and used for first time in Curtin University.

4.2.1 UTS18

The test methods that can be applied to this software included; EN 12697-24: 2004: E (Resistance to fatigue) Annexe D, Four points bending test on prismatic shaped specimens, EN 12697-26: 2004: E (Stiffness) Annex B, Four points bending test on prismatic shaped specimens and finally non-standard testing.

The loading mode is defined as sinusoidal. The major outputs are beam complex modulus, dissipated energy for each cycle, the phase lag between stress and strain, and cumulative dissipated energy. The UTS18 user interface is shown in Figure 4-3

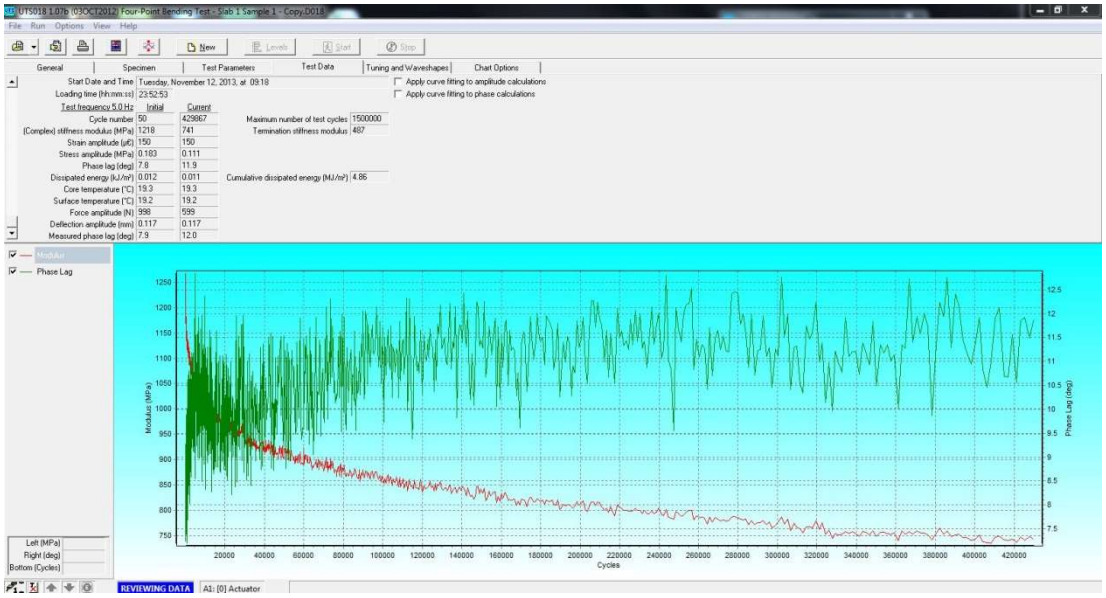

Figure 4-3: UTS18 test layout and description.

4.3 Problems encountered during testing

New apparatus: four-point fatigue test apparatus was a custom made machine that was made for Curtin University. Like any recent innovations in science and technology, this new machine has advantages. This custom made four point apparatus provided this opportunity to study and explore fatigue factors of pavements with sample sizes closer to existing pavements.

Reading the user manual and comparing this apparatus with the standard machine was the only source to give guidance on the machine operation, calibrations and problem solving.

The major problem experienced was that the apparatus stopped working unexpectedly during the test cycle resulting in the failing of two samples. This was reported by Curtin University's laboratory to the manufacturer and rectified.

Another problem encountered was the loss of communication between the apparatus and the computer during the testing procedure that caused sample failure for another two specimens. Air compressor problems were another reason that caused much difficulty in this study.

Heavy samples: With approximately 40kg mass, the large beam samples required careful handling and required two people to move the samples safely and set up in the fatigue apparatus.

Considering the typical values of Young's Elastic Modulus for stabilised material was between 500MPa and 2000MPa, making these samples fragile that could collapse during transportation. Extra caution was taken into account while moving samples.

4.4 Preliminary testing

After performing four trial fatigue tests on a PVC sample in test frequencies of one, two, five and 10 Hz using custom design four-point fatigue test (UTM25) some problems were noted in terms of USB communications dropouts. The way to minimise any dropouts was to ensure that the software was always run with administrative rights.
The output for some of the phase angles was negative, e.g. -120º where the correct value was +60º. This was corrected in the Excel spreadsheet by adding 180 to negative results.

The number of unexpected disconnections from the computer was significantly reduced by running the program as administrator. In term of output the phase angle range in some tests was not in the required range. In this chapter, some solutions will be proposed aiming to overcome the problems.

4.5 Definition of 'validity' and 'reliability'

Validity and reliability are 2 important terms in assessing the results of any experimental program. An illustration of validity and reliability is shown in Figure 4-4.

Figure 4-4: Schematic explanation of validity and reliability (Experiment-resources, 2015)

4.6 Phase lag range

By applying stress to a viscoelastic material a delay occurs before the material dissipates the energy. This lag between the stress and strain is defined as the phase angle. In some tests the output for phase angle is negative, e.g. -170º should be corrected to +10º. This can be

corrected in the Excel spreadsheet by adding 180 to negative results (Asadi, 2015). Figure 4-5 and Figure 4-6 are showing the phase lag and corrected phase lag for a beam respectably.

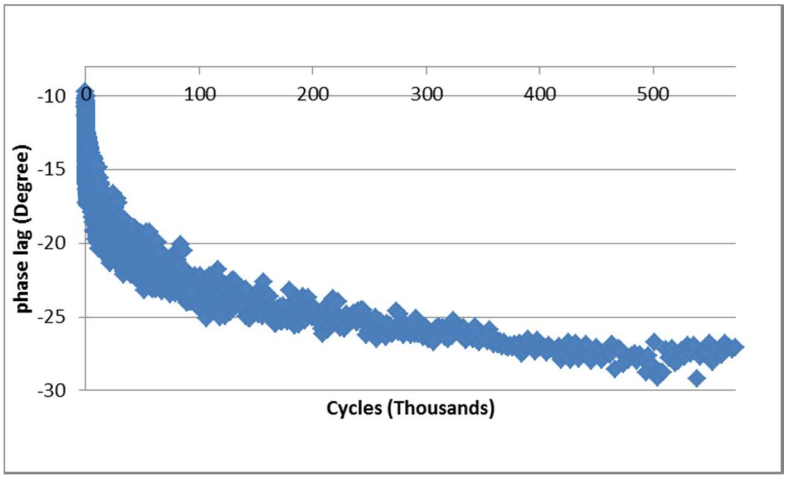

Figure 4-5 : Phase Lag Output

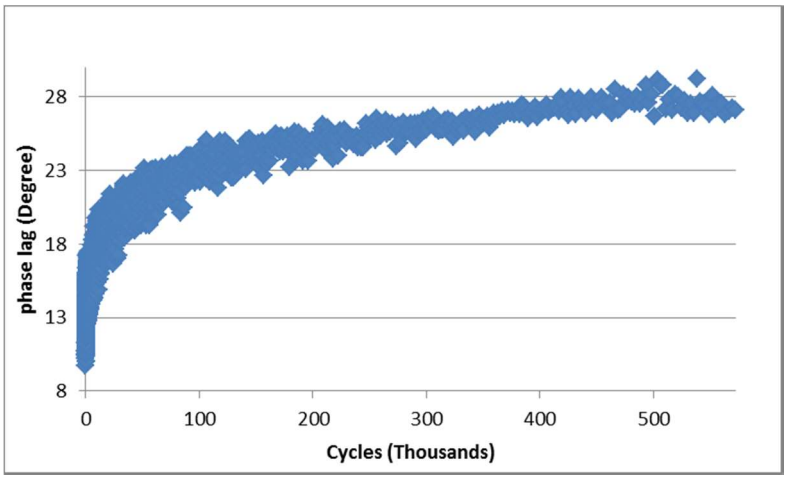

Figure 4-6 : Corrected Phase Lag

5. TEST RESULTS AND ANALYSIS

5.1 Introduction

As explained in previous chapters the scope of the testing program was to evaluate fatigue behaviour of the foamed bitumen stabilised material using the extra-large four-point bending beam apparatus. In this chapter, the results of carried out testings at Curtin University Geomechanics Laboratory are presented and discussed along with an analysis of fatigue life, phase angle, hysteresis loop and dissipated energy. A comparison between determined fatigue life of extra-large beams in the laboratory and calculated fatigue life from fatigue equation provided in AGPT02 (Austroads, 2012) is also presented. Fourteen tests at two frequencies (5 and 10 Hz) at 20°C and different strain levels (100,150 and 200με) were conducted to evaluate the influence of different parameters on fatigue behaviour. The UTS18 software was used to control the testing of large beams. The properties of the large beam samples and test conditions are presented in Table 5-1.

Table 5-1: Properties of samples and testing conditions

Sample number	Dimensions (mm)	Strain level (με)	Frequency (Hz)	Testing temperature (°C)
1	180.3×149.8×820	150	5	20
2	179.3×144.4×815	150	5	20
3	180.4×150.5×812	150	5	20
4	181.8×149.5×820	200	10	20
5	182.7×143.8×820	200	10	20
6	179.5×150.8×825	200	10	20
7	182.3×151.7×825	200	10	20
8	179.2×144.6×825	100	5	20
9	181.7×147×816.5	100	5	20
10	180.3×149.8×820	150	5	20
11	180×143.1×822.5	100	5	20
12	185×140.2×802.5	100	5	20
13	180.4×150.3×817.5	100	5	20
14	186.6×142.2×822.5	100	5	20

As previously mentioned in Chapter 3 Two slabs were retrieved from the in-service pavements. Following are the details of each slab location:

- Slab 1 from Kewdale Road base material containing foamed bitumen.
- Slab 2 from Nicholson Road base material containing crushed rehabilitated asphalt and

foamed bitumen.

The slabs were cut into beams in the laboratory and numbered from 1 to 14 where samples 1–10 belong to the slab 1 and samples 11– 14 belong to slab 2. All test results on beam samples are presented in Appendix A.

5.2 Fatigue life determination

The termination conditions for fatigue testing using four-point bending beam apparatus are defined as follows:

- When the testing sample reaches it's 50% initial stiffness,
- or after application of the previously defined number of loading cycles (e.g. 1,500,000).

In this study, the only test on sample 2 terminated according to the abovementioned criteria. Based on this it was necessary to extrapolate the fatigue life by fitting the best curve to the fatigue results. Table 5-2 outlines the testing samples which need extrapolation to determine their fatigue life.

Table 5-2: Percent stiffness reduction for terminated and unterminated fatigue tests

Sample number	Terminated		Stiffness reduction (%)
	Yes	No	
1		✓	39.15%
2	✓		50.75%
4		✓	39.89%
8		✓	40.20%
9		✓	20.65%
10		✓	27.59%
11		✓	18.85%
12		✓	32.53%
13		✓	49.52%
14		✓	NA
3, 5, 6 & 7[a]	–	–	–

[a] It should be noted that sample 3 and 6 damaged during transportation due to the large size and heavy weight. Also, sample 5and 7 test results are excluded from analysis due to the apparatus error.

As it was explained in Table 5-2 some of the samples were damaged during the testing process which resulted in erroneous test results. The concept of validity and reliability has been used and these results deleted from this study. Figure 5-1 is an example of erroneous test results where the trend in stiffness reduction is not detectable.

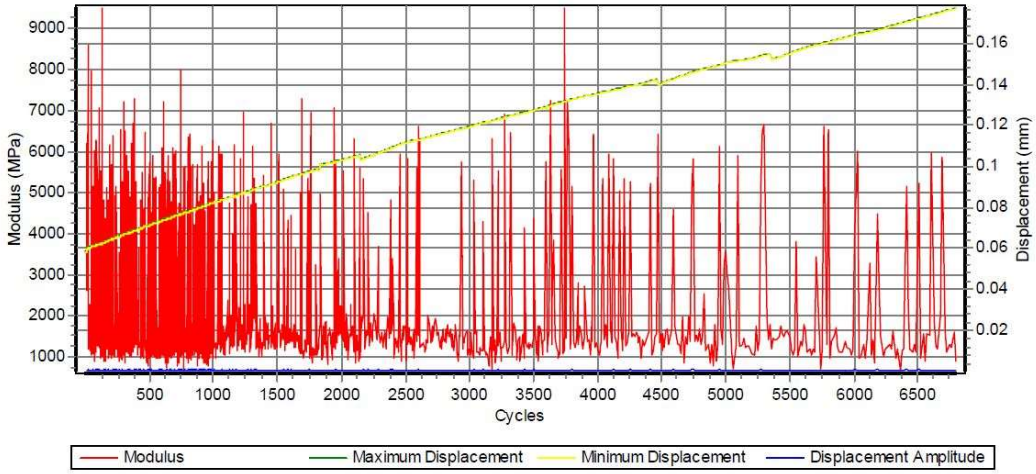

Figure 5-1: Erroneous fatigue test results for sample number 5

5.2.1 Curve fitting

To fit the best curve to the test results after significant research the method proposed by Asadi (Asadi, 2015) was adopted. This method uses a logarithmic equation for curve fitting purpose and represented in Equation 5-1 as follows:

$$E = \alpha\big(ln(\beta N + \gamma)\big) + E_{max} \qquad 5\text{-}1$$

Where

E = material stiffness (MPa)

N = number of load cycle during testing

$\alpha, \beta \,\&\, \gamma$ = curve fitting parameters

E_{max} = maximum theoretical stiffness (MPa)

As it is apparent from Equation 5-1 there are some fitting parameters which should be determined before plotting the modelled fatigue curve. Using Microsoft Excel® Solver Analysis Tool was suggested by Asadi (Asadi, 2015) to determine these parameters. Table 5-3 is an example of curve fitting procedure.

Table 5-3: Example of excel file to determine fitted curve and fatigue life.

A	B	C	D
Cycle number	Stiffness (MPa)		(B-C)^2
	Fatigue Results	Fitted Curve	
50	410.496	558.374	21868.01
51	421.145	557.982	18724.39
52	418.436	557.597	19365.81
53	415.582	557.219	20061.09
54	418.857	556.848	19041.52
55	422.037	556.483	18075.83
56	419.289	556.125	18724.11
57	408.367	555.772	21728.49
58	413.136	555.426	20246.6
59	420.969	555.085	17987.35
60	415.167	554.750	19483.64
.	.	.	.
.	.	.	.
.	.	.	.
N_n	E	E_n	$(B_n-C_n)^2$

The following procedure was used to determine the curve fitting parameters (see also Table 5-4):

Step 1. An initial value for a, β, γ and E_{max} should be defined (E_{max} is defined as the initial stiffness).

Step 2. The loading cycles and the recorded stiffness during the test should be located in column A and B progressively.

Step 3. Using the Equation 5-1the modelled stiffness should be placed in column C.

Step 4. The square of errors should be placed in column D.

Step 5. Using Microsoft Excel® Solver Analysis Tool the summation of square errors should be minimised.

Step 6. The final fitting parameters and the goodness of fit for the curve (R^2) should be recorded.

Figure 5-4 is a summary of the fitting parameters for each sample beam after following the above-mentioned steps for curve fitting.

Table 5-4: Fitting parameters of tested beam samples

Sample number	Fitting parameters				R^2	Terminated		Stiffness reduction (%)
	α	γ	β	E_{max}		Yes	No	
1	-54.51	0.20	64.98	1722.05	0.983		✓	39.15%
2	-56.82	16741.19	4.45	1295.265	0.959	✓		50.75%
4	-35.54	145989.81	8007.47	1383.235	0.949		✓	39.89%
8	-42.01	0.20	65.31	1416.91	0.987		✓	40.20%
9	-38.16	0.20	63.94	2249.62	0.983		✓	20.65%
10	-29.18	53335.72	2.90	861.70	0.965		✓	27.59%
11	-20.70	145.00	66.29	727.06	0.962		✓	18.85%
12	-8.55	68.29	87.03	339.93	0.884		✓	32.53%
13	-18.82	179.82	54.86	532.94	0.991		✓	49.52%
14	-2.21	261.21	27.35	252.83	NA		✓	NA

Figure 5-2 to Figure 5-11 show the fitted curves on the fatigue test results based on the process which has been explained above.

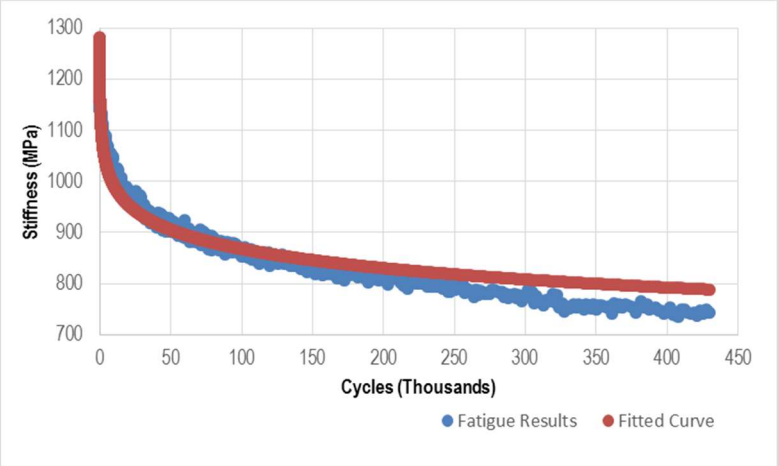

Figure 5-2: Fitted curve for sample number 1

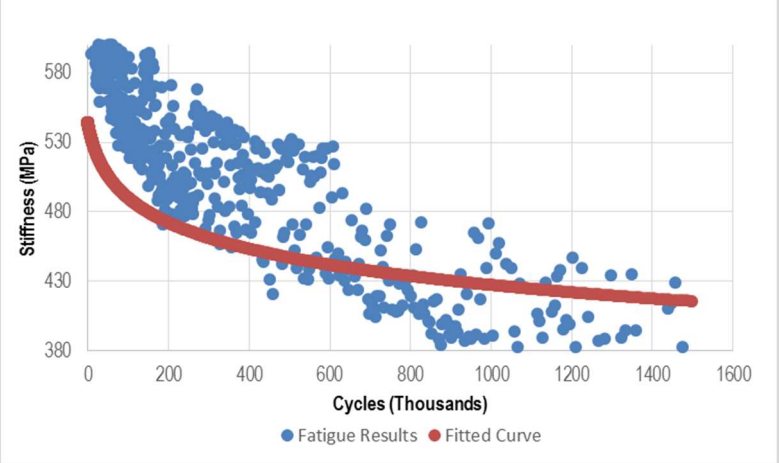

Figure 5-3: Fitted curve for sample number 2

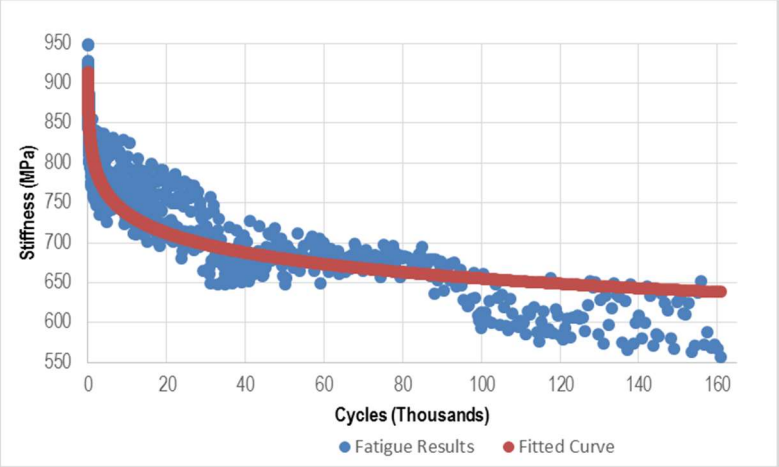

Figure 5-4: Fitted curve for sample number 4.

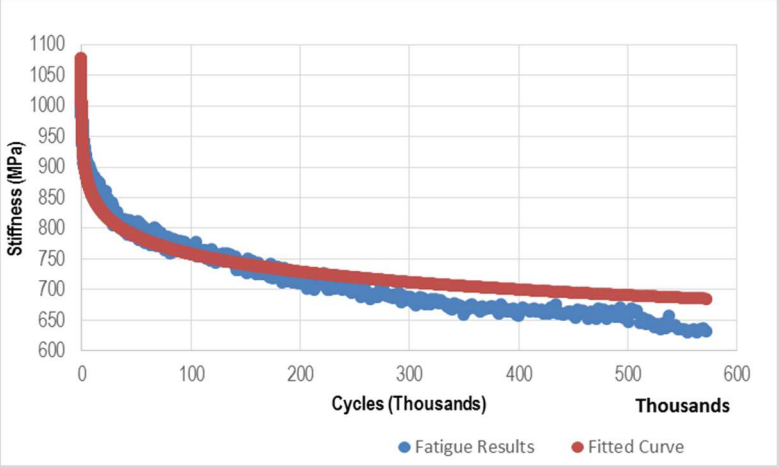

Figure 5-5: Fitted curve for sample number 8.

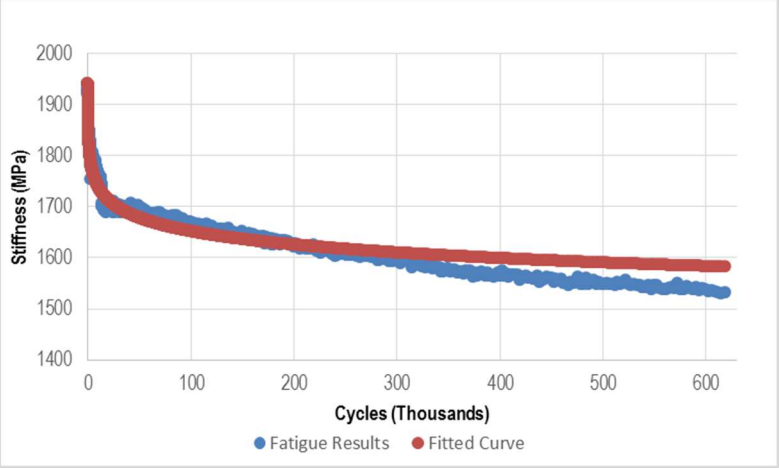

Figure 5-6: Fitted curve for sample number 9.

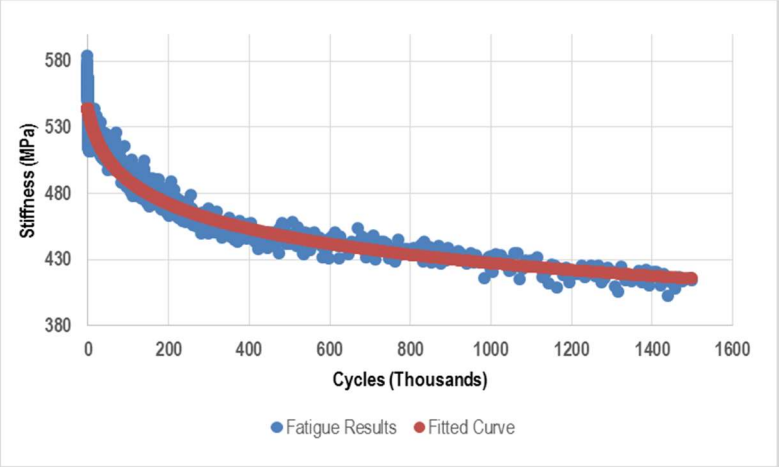

Figure 5-7: Fitted curve for sample number 10

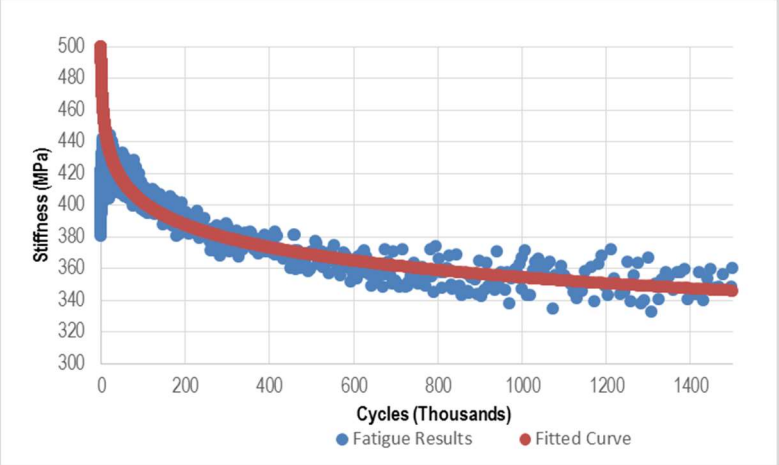

Figure 5-8: Fitted curve for sample number 11

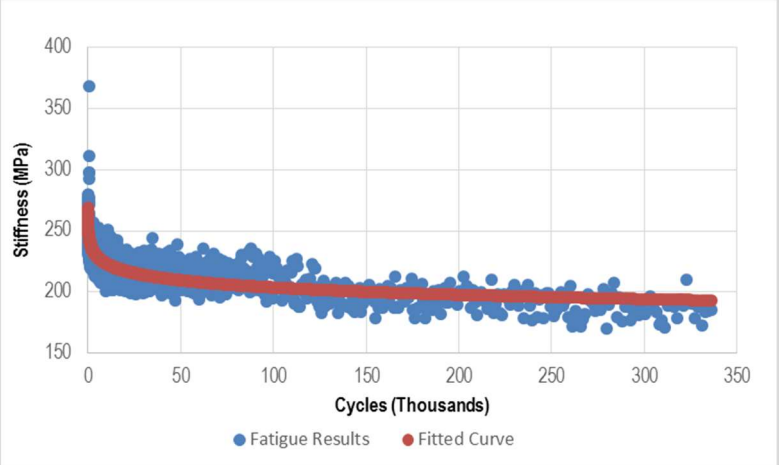

Figure 5-9: Fitted curve for sample number 12.

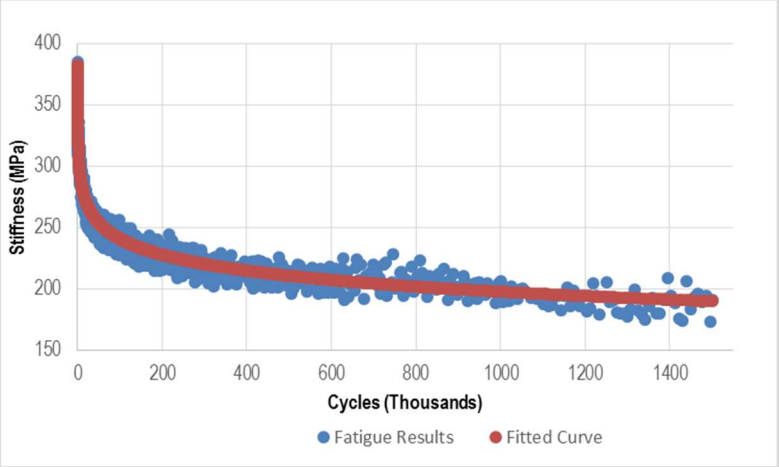

Figure 5-10: Fitted curve for sample number 13

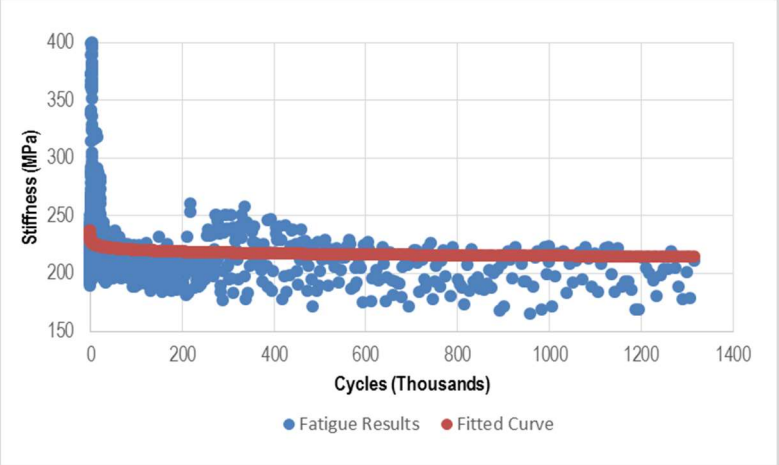

Figure 5-11: Fitted curve for sample number 14.

5.2.2 Extrapolation of fatigue life

As explained before the majority of the tests have not met the termination condition. For this reason, the fatigue life should be extrapolated. After curve fitting process to determine the fatigue life an extrapolation method suggested by Asadi (Asadi, 2015) was utilised. In this method an adjustment factor compatible with the terminated stiffness multiplied to initial stiffness in Equation 5-1 and the formula adjusted to Equation 5-2 as follows:

$$N_f = \frac{e^{\left(\frac{\emptyset Ei - 2Emax}{2\alpha}\right) - \delta}}{\beta} \qquad 5\text{-}2$$

Where

$\emptyset$ = Adjustment Factor

Table 5-5 represents the adjustment factors proposed by Asadi (Asadi, 2015) for fatigue life prediction.

Table 5-5: Template adjustment factor for diffrent stiffnesses reduction states (Asadi, 2015)

Stiffness Loss (%)	Adjustment factors (Φi)			STD	% Stiffness	Adjustment factors (Φi)			STD
	Max	Min	Average		Loss	Max	Min	Average	
43.5	1.1788	1.2625	1.1264	0.0489	25	1.2809	1.3523	1.2307	0.0556
43	1.1816	1.2661	1.1318	0.049	24.5	1.2838	1.3523	1.2315	0.0559
42.5	1.185	1.2693	1.1358	0.0491	24	1.2877	1.3574	1.2329	0.0567
42	1.1878	1.2694	1.1399	0.049	23.5	1.2902	1.3575	1.234	0.0564
41.5	1.1909	1.2727	1.1438	0.0494	23	1.2922	1.3575	1.2351	0.0564
41	1.1935	1.2758	1.1477	0.0492	22.5	1.2944	1.3598	1.236	0.0567
40.5	1.1965	1.279	1.1528	0.0494	22	1.2967	1.3599	1.2367	0.0564
40	1.1995	1.2821	1.1565	0.0493	21.5	1.2994	1.3649	1.2369	0.0566
39.5	1.202	1.2851	1.1601	0.0494	21	1.301	1.3649	1.2373	0.0564
39	1.2044	1.2852	1.1636	0.049	20.5	1.3034	1.365	1.2384	0.0561
38.5	1.2077	1.29	1.1682	0.0493	20	1.3058	1.365	1.2406	0.0551
38	1.2101	1.2901	1.1715	0.0488	19.5	1.3092	1.3683	1.2436	0.055
37.5	1.2134	1.2957	1.1758	0.0497	19	1.3119	1.3705	1.247	0.0547
37	1.2156	1.2957	1.1789	0.0494	18.5	1.3159	1.3706	1.2508	0.0522
36.5	1.2181	1.2994	1.1829	0.0495	18	1.3192	1.3706	1.2553	0.0508
36	1.221	1.3034	1.1867	0.05	17.5	1.3234	1.3748	1.2593	0.0493
35.5	1.2234	1.3036	1.1894	0.0495	17	1.3267	1.3747	1.2644	0.0482
35	1.2263	1.3086	1.1929	0.0502	16.5	1.3307	1.3747	1.2694	0.0453
34.5	1.2285	1.3087	1.1962	0.0501	16	1.3331	1.3749	1.2743	0.0438
34	1.231	1.3115	1.1994	0.05	15.5	1.3264	1.3775	1.2788	0.0419
33.5	1.2339	1.3115	1.2031	0.0498	15	1.3303	1.3797	1.2831	0.0406
33	1.2376	1.3178	1.2058	0.0511	14.5	1.335	1.3834	1.2887	0.0378
32.5	1.2401	1.3179	1.2091	0.0505	14	1.3388	1.3839	1.2939	0.0358
32	1.243	1.3216	1.2123	0.0513	13.5	1.343	1.3835	1.2999	0.0329
31.5	1.2454	1.3217	1.2153	0.051	13	1.3484	1.3851	1.3041	0.0294
31	1.2485	1.3257	1.2174	0.0519	12.5	1.3537	1.3924	1.3093	0.0285
30.5	1.2511	1.3259	1.2186	0.0519	12	1.3607	1.3969	1.3147	0.0263
30	1.254	1.3305	1.2199	0.0528	11.5	1.3662	1.3982	1.3201	0.0264
29.5	1.2569	1.3335	1.2213	0.0532	11	1.3707	1.3988	1.3249	0.0264
29	1.2594	1.3335	1.2222	0.0536	10.5	1.3739	1.4036	1.329	0.0271
28.5	1.2614	1.3336	1.2235	0.0535	10	1.3807	1.4118	1.3249	0.0304
28	1.2645	1.3375	1.2247	0.0542	9.5	1.3878	1.4351	1.3017	0.0394
27.5	1.2668	1.3377	1.2258	0.0544	9	1.3935	1.4458	1.2994	0.043
27	1.2704	1.3428	1.2268	0.0551	8.5	1.3955	1.45	1.2983	0.0505
26.5	1.2724	1.343	1.2278	0.0548	8	1.4013	1.45	1.2934	0.0548
26	1.2748	1.3474	1.2284	0.0552	7.5	1.4085	1.4677	1.2587	0.0678
25.5	1.2776	1.3475	1.2293	0.0548	7	1.4253	1.484	1.1456	0.1021
					6.5	1.4338	1.5132	1.0054	0.1496

Figure 5-12 shows an example of extrapolated curve to the 50% stiffness reduction on fatigue test results for sample number 1.

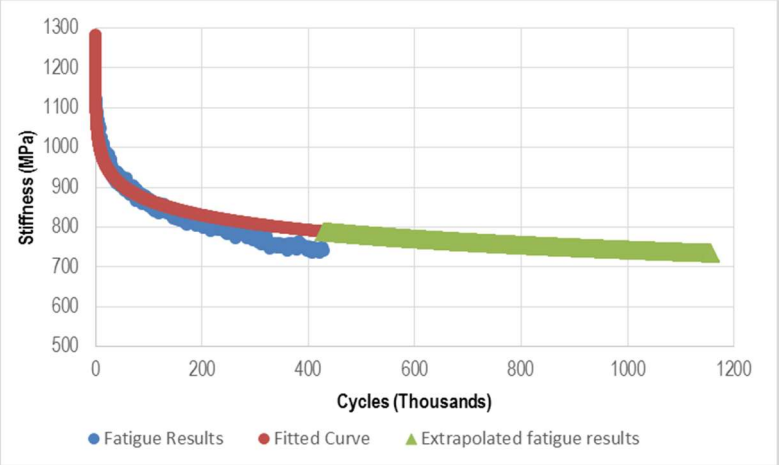

Figure 5-12: Extrapolated fatigue curve for sample number 1

Predicted fatigue lives using the extrapolation methodology proposed by Asadi, 2015 are summarised in Table 5-6.

Table 5-6: Extrapolate fatigue life for the tested samples

Sample number	Initial stiffness	Recorded		Stiffness reduction (%)	Used adjustment factor	Recorded number of test cycles in the laboratory	Estimated fatigue life
		Cycles	Final stiffness				
1	1218	429,867	741	39.15%	1.20	429,867	1,157,316
2	738	1,500,000	362	50.75%	1	1,500,000	2,751,168
4	926	160,941	557	39.89%	1.19	160,941	1,618,457
8	1054	572,504	631	40.20%	1.19	572,504	2,010,140
9	1931	657,322	1,287	20.65%	1.30	657,322	3,107,476,739
10	571	1,500,000	414	27.59%	1.26	1,500,000	9,418,027
11	410	1,500,000	360	18.85%	1.31	1,500,000	60,334,403
12	275	336,254	185	32.53%	1.24	336,254	30,823,901
13	378	1,500,000	190.889	49.52%	1	1,500,000	1,567,361
14	204	1,316,572	210.584	39.15%	NA	1,316,572	NA

5.3 Phase angle results

Due to viscous nature of the viscoelastic materials (e.g. hot mix asphalt), their respond to the loading is time dependent which means there is a delay between stress and strain and it takes some time for the material to dissipate the energy after loading. This lag between the stress and strain is defined as the phase angle. The maximum theoretical value for the phase angle is 90º for a totally viscous material and the minimum theoretical value is 0º for a totally elastic material.

The recorded phase lag for each tested sample during the fatigue testing is plotted against the recorded cycles and shown in Figure 5-13 to Figure 5-22.

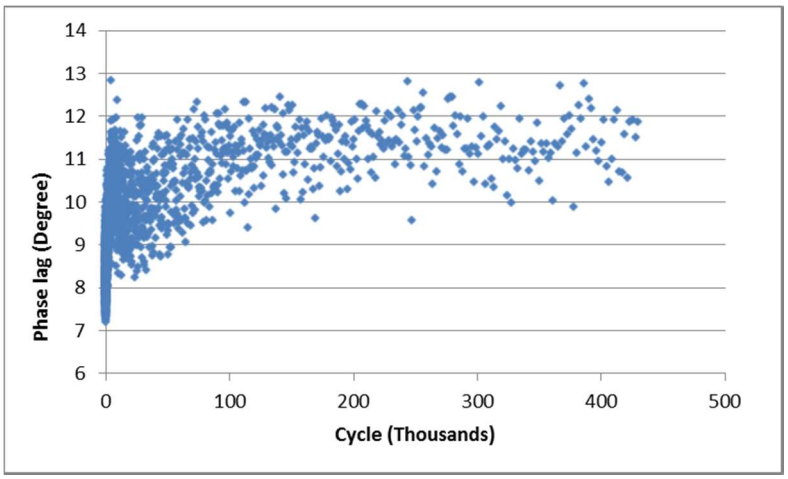

Figure 5-13: Phase lag, sample number 1

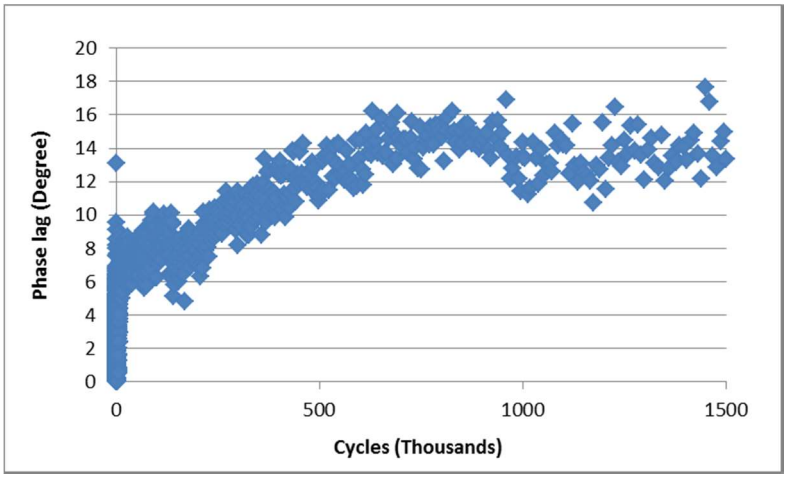

Figure 5-14: Phase lag, sample number 2

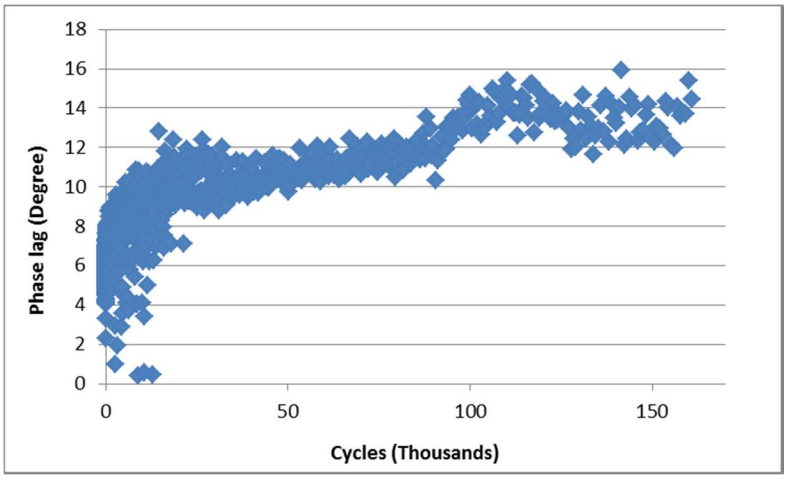

Figure 5-15: Phase lag, sample number 4

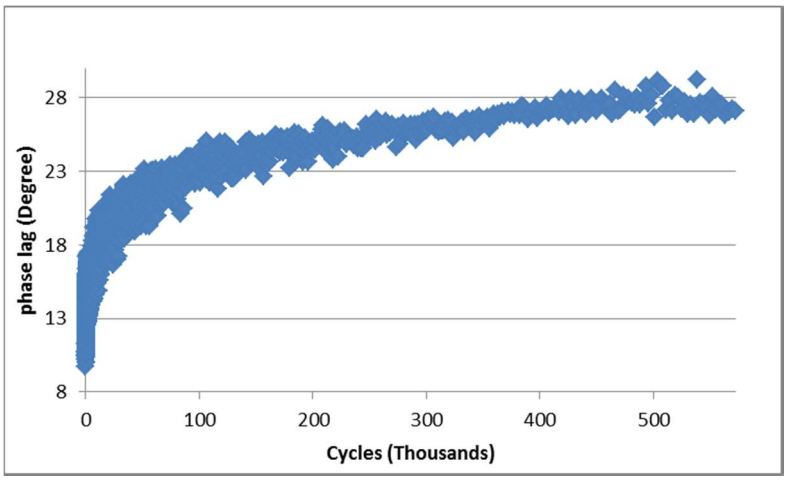

Figure 5-16: Phase lag, sample number 8

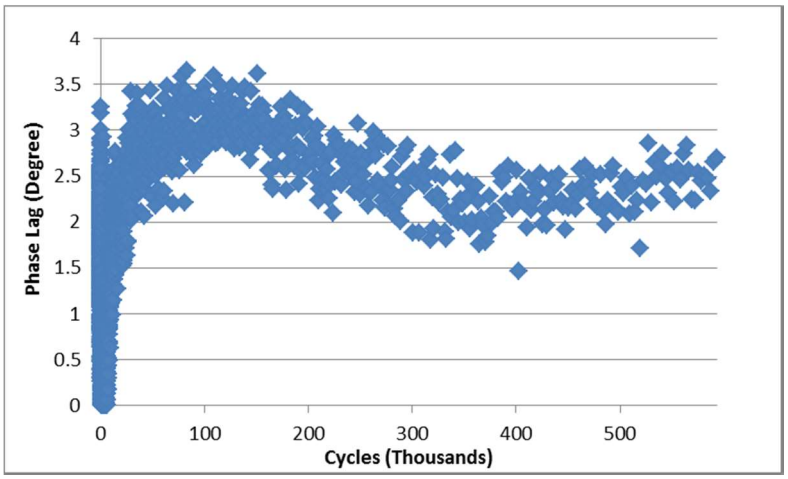

Figure 5-17: Phase lag, sample number 9

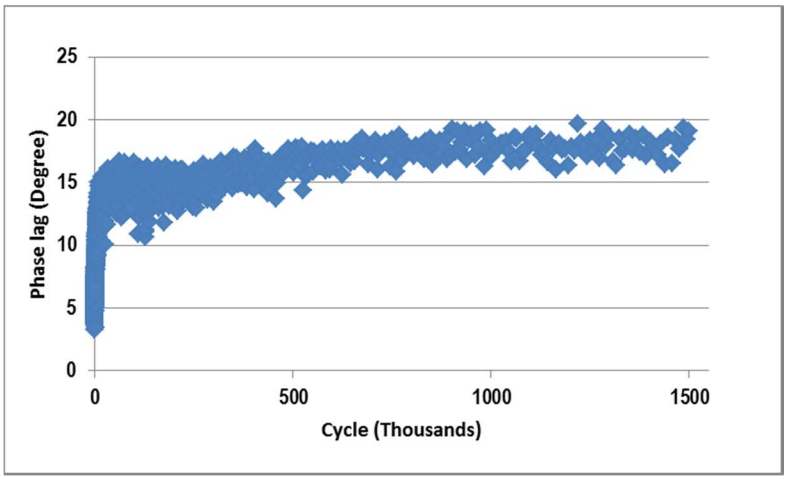

Figure 5-18: Phase lag, sample number 10

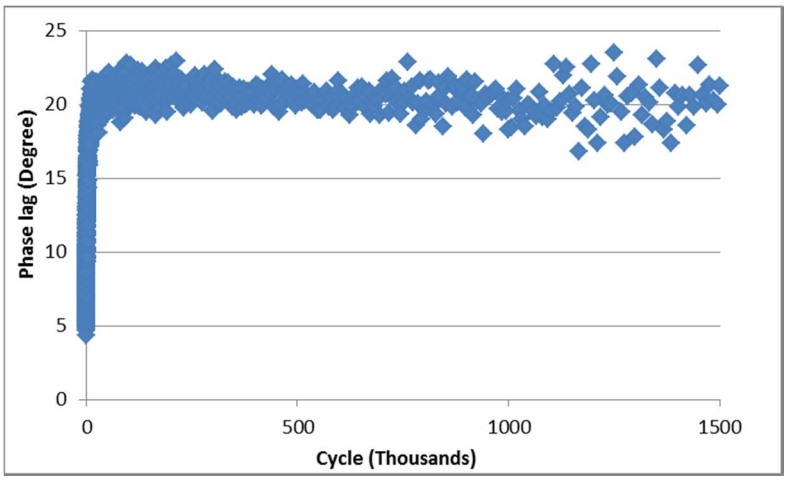

Figure 5-19: Phase lag, sample number 11

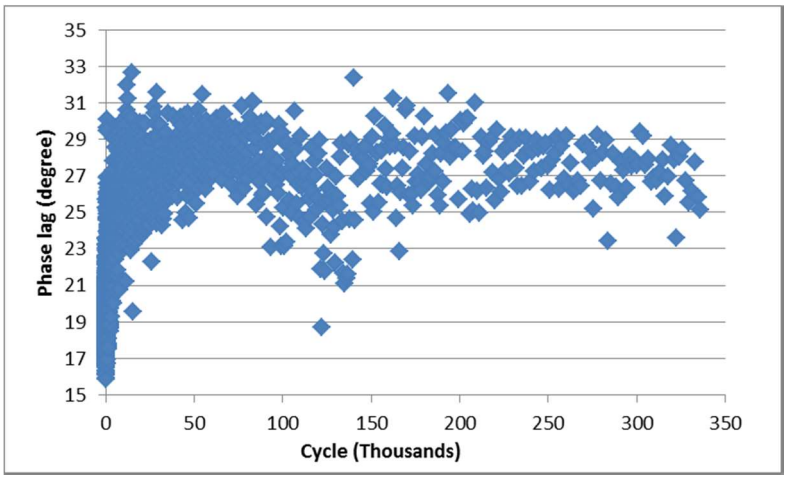

Figure 5-20: Phase lag, sample number 12

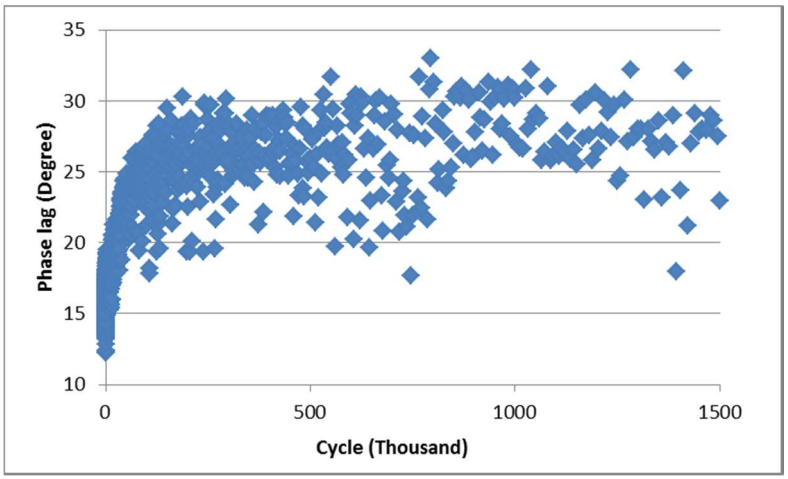

Figure 5-21: Phase lag, sample number 13

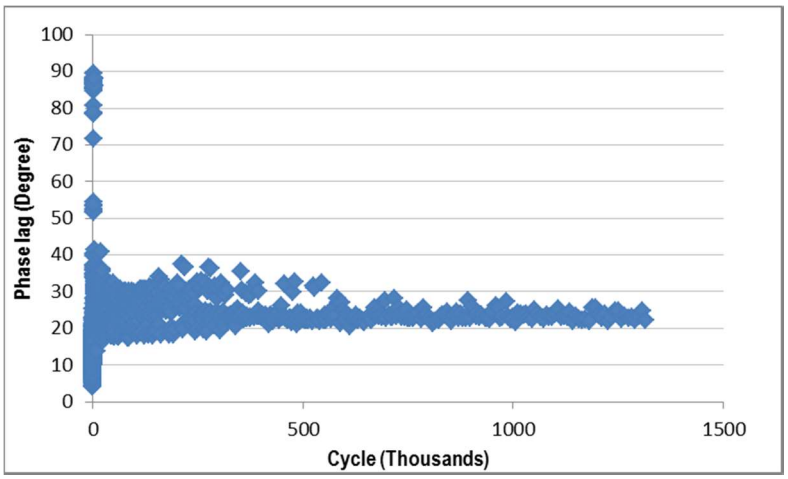

Figure 5-22: Phase lag, sample number 14

Table 5-7 is a summary of recorded phase angle ranges for tested beams, after 100 thousand loading cycles. As it is apparent from Table 5-7 the phase angle ranges for samples which were retrieved from Slab 1 are lower compared to those from Slab 2. This indicates that the behaviour of Slab 1 samples is more elastic whereas the behaviour of those from Slab 2 is more viscoelastic. It should be noted that the Slab 2 has more bitumen content than Slab 1. This confirms the concept that adding more bitumen as viscous additive results in viscoelastic performance of the material

Table 5-7: Recorded phase angle range after 100 thousand cycles (Degree) for beam samples

Slab No	Bitumen Content by volume (%)	Sample No	Phase angle ranges after 100 thousand cycles (Degree)
1	4.1	1	10–13
		2	10–18
		4	10–18
		8	18–29
		9	2–4
		10	10–20
2	6.6	11	16–25
		12	21–31
		13	20–32
		14	NA

5.4 Hysteresis loop and dissipated energy

A material's ability to absorb energy without fracturing is directly related to crack development of that material. The dissipated energy per load cycle can be calculated as the area of the hysteresis loop generated by four-point bending beam testing machine. The hysteresis loops for initial loading cycle and also for the last loading cycle for the samples

extracted from Slab 1 are plotted in Figure 5-23 to Figure 5-28 and Figure 5-29 to Figure 5-32 for those extracted from Slab 2.

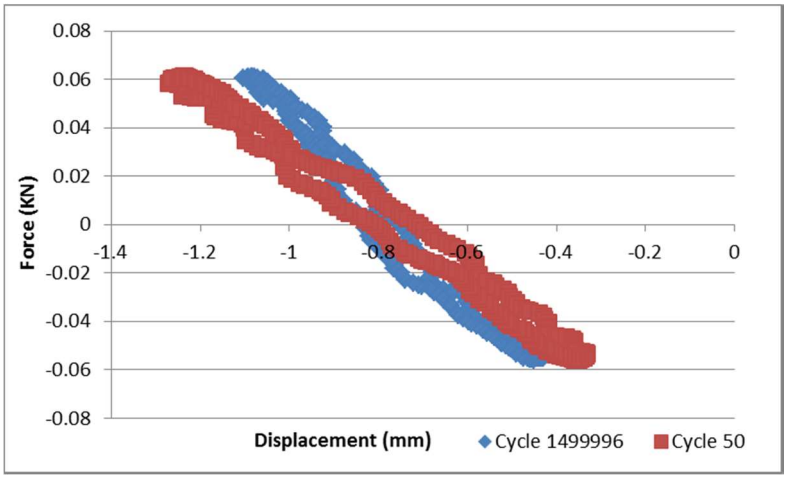

Figure 5-23: Hysteresis loops for sample number 1

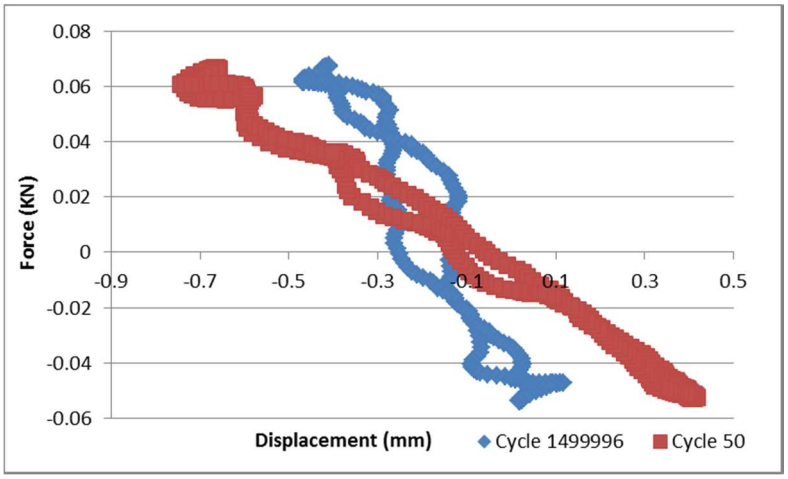

Figure 5-24: Hysteresis loops for sample number 2

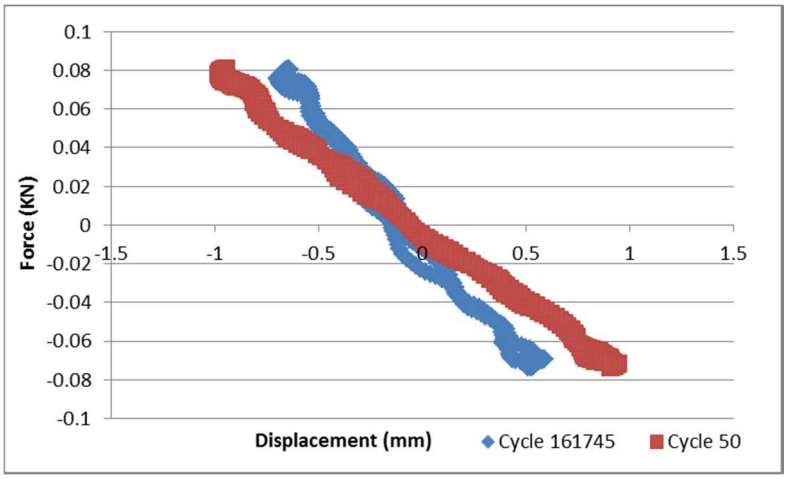

Figure 5-25: Hysteresis loops for sample number 4

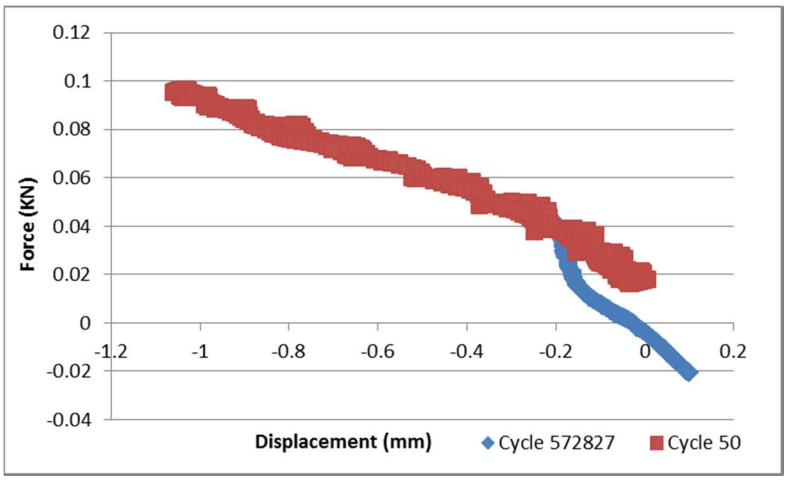

Figure 5-26: Hysteresis loops for sample number 8

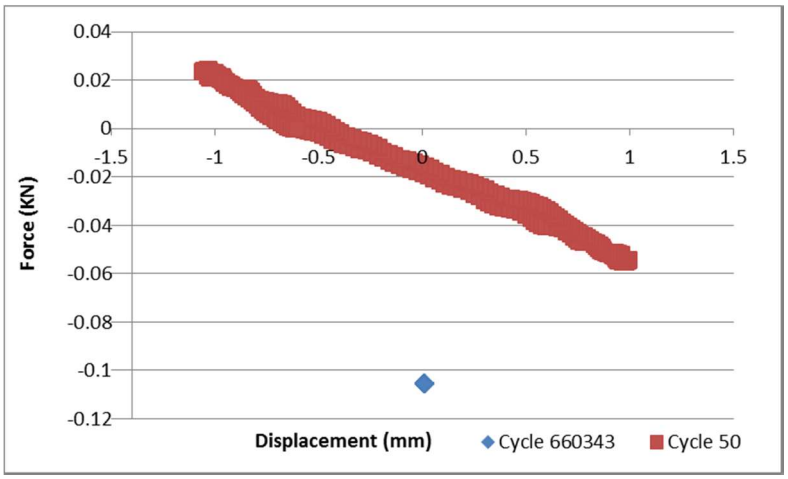

Figure 5-27: Hysteresis loops for sample number 9

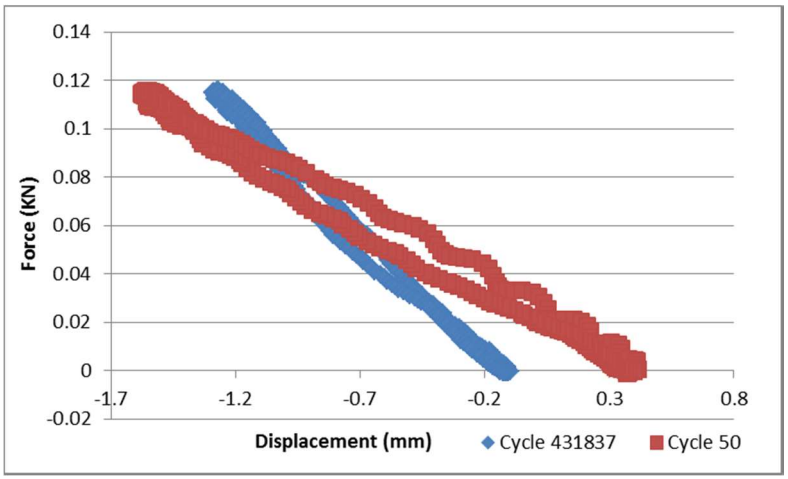

Figure 5-28: Hysteresis loops for sample number 10

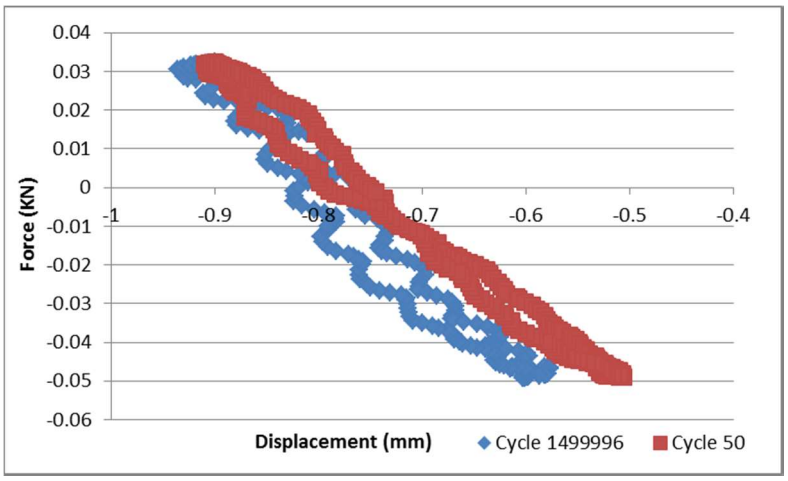

Figure 5-29: Hysteresis loops for sample number 11

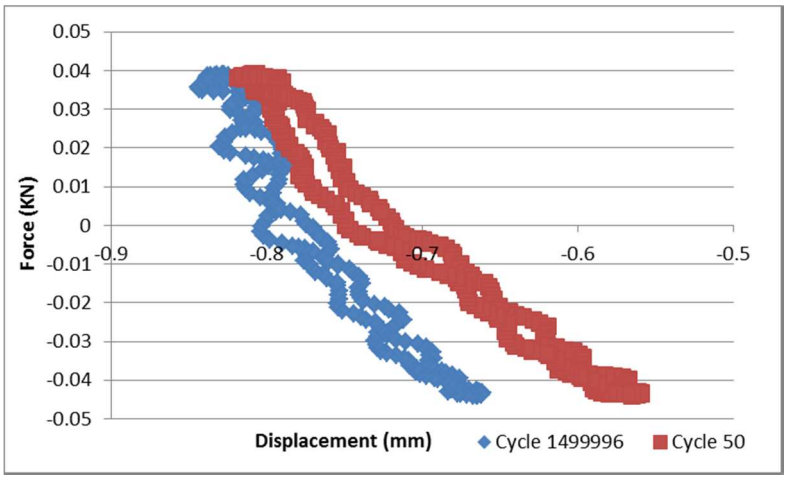

Figure 5-30: Hysteresis loops for sample number 12

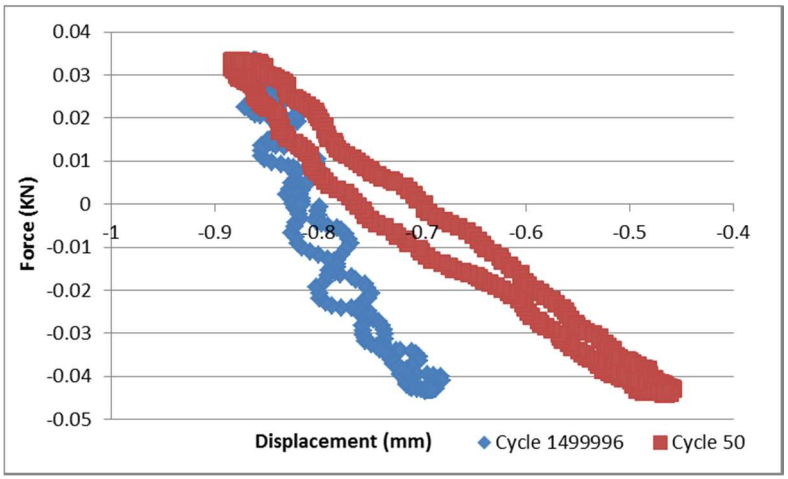

Figure 5-31: Hysteresis loops for sample number 13

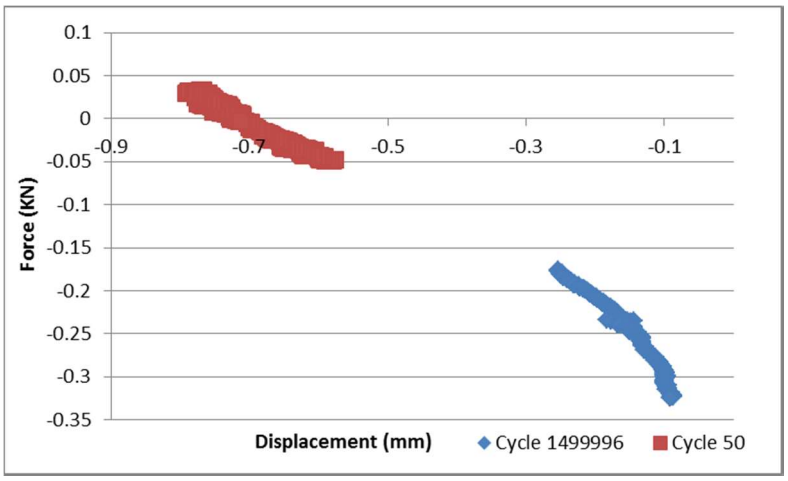

Figure 5-32: Hysteresis loops for sample number 14

It can be seen from Figure 5-23 to Figure 5-32 that the hysteresis loop shapes of samples extracted from Slab 1 resemble line while the shape of the hysteresis loops for the ones extracted from Slab 2 are more elliptical. This again confirms the elastic behaviour of Slab 1 materials and viscoelastic behaviour of Slab 2 materials which has higher binder content. Figure 5-33 and Figure 5-34 summarise the hysteresis loop results for initial and last loading cycles of samples retrieved from Slab 1 whereas Figure 5-35 and Figure 5-36 represent the recorded hysteresis loops for initial and last loading cycles of the samples extracted from Slab 2.

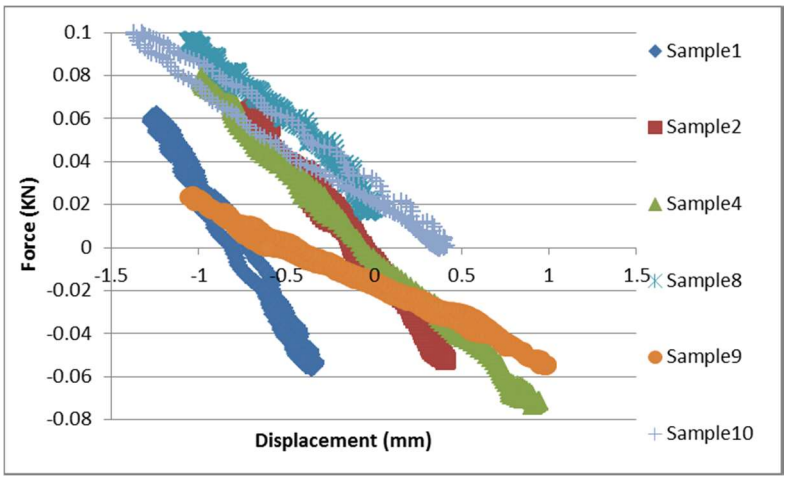

Figure 5-33: Hysteresis loops for initial cycle (Slab 1)

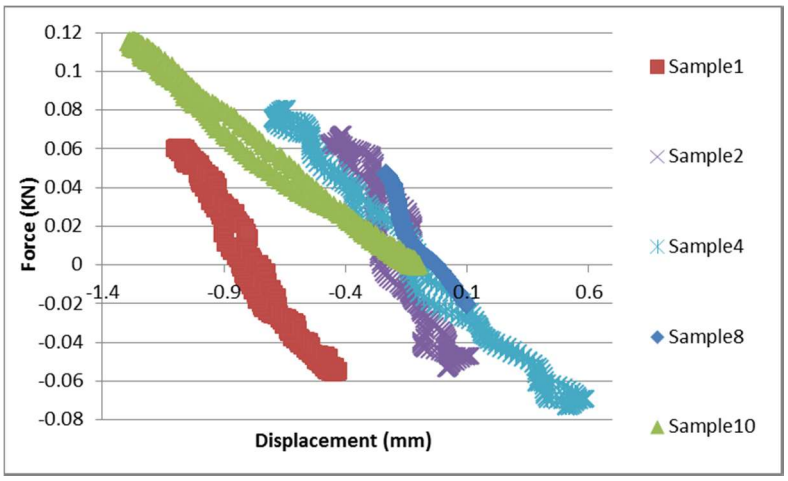

Figure 5-34: Hysteresis loops for the last cycle (Slab 1)

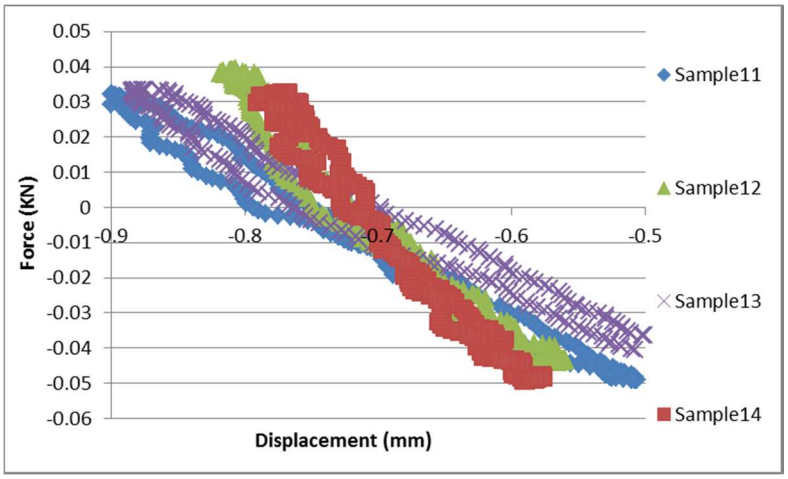

Figure 5-35: Hysteresis loops for initial cycle (Slab 2)

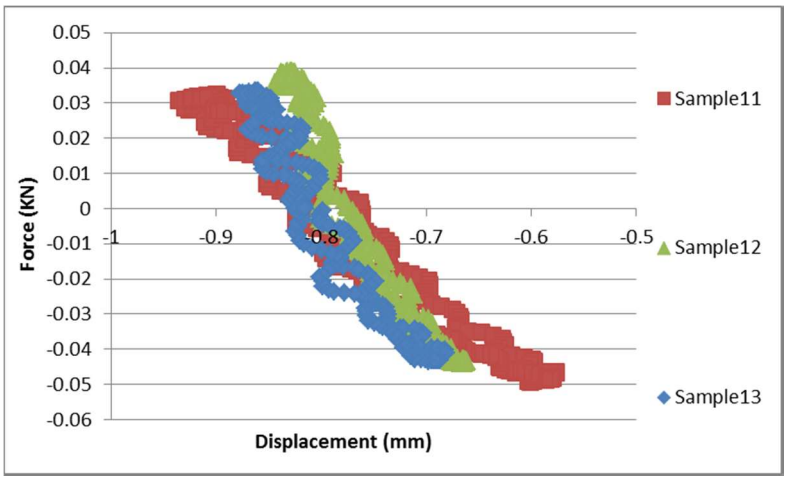

Figure 5-36: Hysteresis loops for the last cycle (Slab 2)

As mentioned before the area of hysteresis loop equals to the dissipated energy of loading cycle. Although Slab 2 performs as a viscoelastic material due to its high binder content, the samples extracted from Slab1 show a larger area of the hysteresis loop. This could be better

explained by dissipated energy concept. For this reason, the average, maximum, minimum and standard deviation (STD) of all recorded cycles are represented in Figure 5-37 for the samples cut from Slab 1 and in Figure 5-38 for the ones extracted from Slab 2.

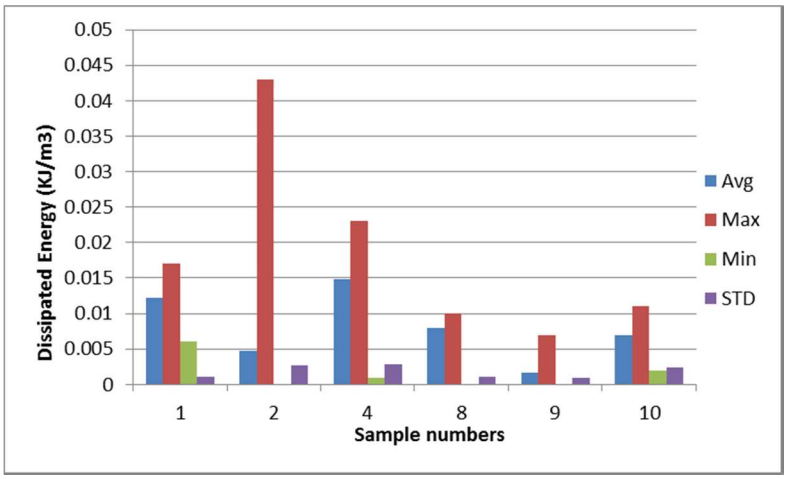

Figure 5-37: Dissipated Energy for slab number 1

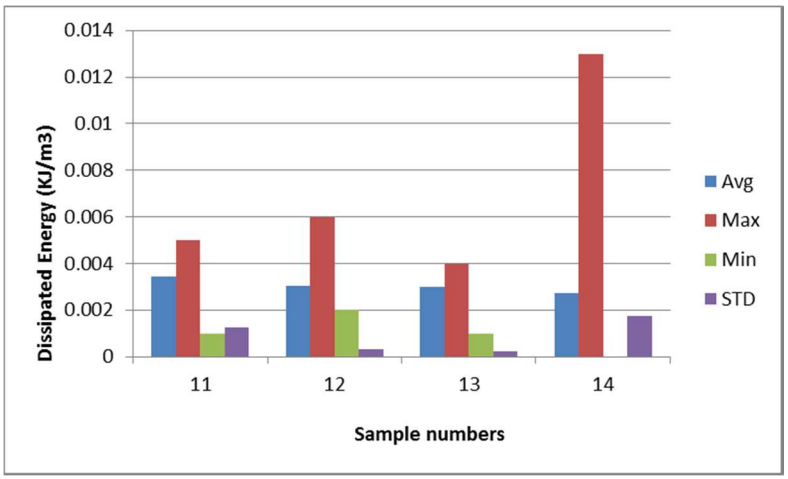

Figure 5-38: Dissipated Energy for slab number 2

It can be seen from Figure 5-37 and Figure 5-38 that the dissipated energy values are higher for Slab 1 compare to Slab 2. As the average flexural stiffness of Slab1 is higher than Slab 2 larger force should be applied to the beams to maintain the constant strain during four-point bending beam testing which results in higher dissipated energy for each loading cycle. The average flexural stiffness of Slab 1 and Slab 2 are represented in Table 5-8.

Table 5-8: Average initial stiffness for each slab

Slab number	Average initial stiffness (MPa)	Binder content by volume (%)
1	1073	4.1
2	317	6.6

For comparison purposes, the cumulative dissipated energy of each tested beam is also plotted against the testing cycles and presented in Figure 5-39. It is apparent the cumulative energy value is higher in average for Slab 1 (Sample 1 to Sample 10) compared to Slab 2 (Sample 11 to Sample 14) due to the same aforementioned reason.

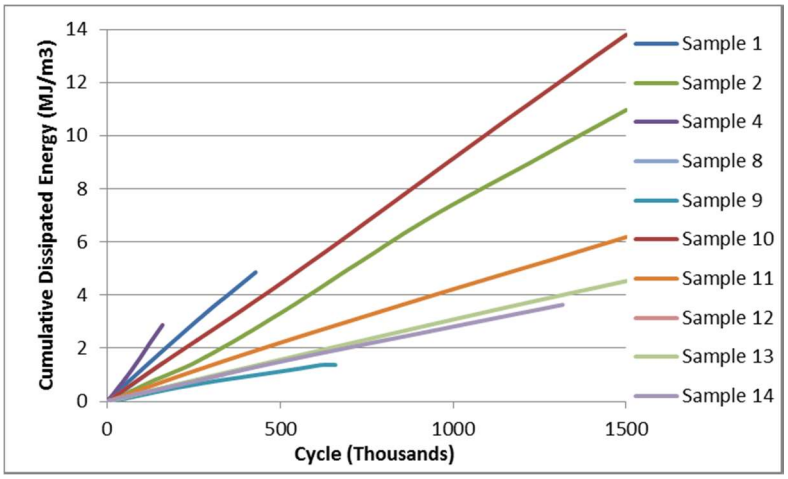

Figure 5-39: Cumulative Dissipated Energy (MJ/m3)

5.5 Comparing the determined fatigue life from the laboratory with Austroads fatigue equation

As explained in Chapter 1, Equation 1-1 provided in AGPT02 (Austroads 2012) to determine the in-situ fatigue life of asphalt materials. The Reliability Factors for the desired project reliability published in AGPT02 (Austroads, 2012) are shown in Table 5-9.

Table 5-9: Reliability factors for desired project reliability (Austroads 2012)

Desired project reliability				
80%	85%	90%	95%	97.5%
2.5	2	1.5	1	0.67

In this study, a reliability factor of 1 is considered as the slabs were retrieved from an urban highway with the desired project reliability of 95%. The comparison between laboratory determined fatigue lives and Austroads fatigue equation is summarised in Table 5-10.

Table 5-10: fatigue life comparison between laboratory test results and AGPT02 fatigue equation

Sample number	Initial flexural stiffness (MPa)	Estimated fatigue life (cycles)	
		Laboratory	AGPT02
1	1218	1,157,316	1,186,194
2	738	2,751,168	2,922,935
4	926	1,618,457	461,028
8	1054	2,010,140	11,685,946
9	1931	3,107,476,739	3,929,786
10	572	9,418,027	4,630,303
11	410	60,334,403	433,349,302
12	275	30,823,901	889,303,895
13	378	1,567,361	508,853,495
14	204	NA	1,522,350,808

The laboratory determined fatigue life of samples 1 and 2 were very close to the Austroads equation whilst samples number 4, 9 and 10 show significantly higher fatigue lives when compared to the ones determined from the AGPT02 (Austroads, 2012) fatigue equation. It was also noticed that sample 8 shows smaller fatigue life in the laboratory compare to determine fatigue life from AGPT02 (Austroads, 2005) equation. The estimated fatigue lives from laboratory results against AGPT02 (Austroads, 2012)b fatigue equation for Slab 1 are plotted in Figure 5-40

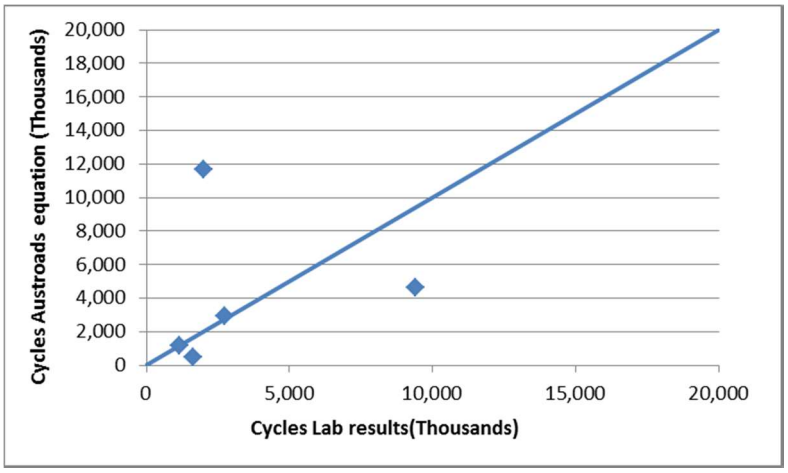

Figure 5-40: Fatigue life from laboratory test against Austroads fatigue equation for slab 1

The laboratory estimated fatigue lives results were also significantly lower than the ones determined from the AGPT02 (Austroads, 2012) fatigue equation. The estimated fatigue lives from laboratory results against AGPT02 (Austroads, 2012) fatigue equation for Slab 1 are plotted in Figure 5-40. Fatigue equation for Slab 2 are plotted in Figure 5-41.

.

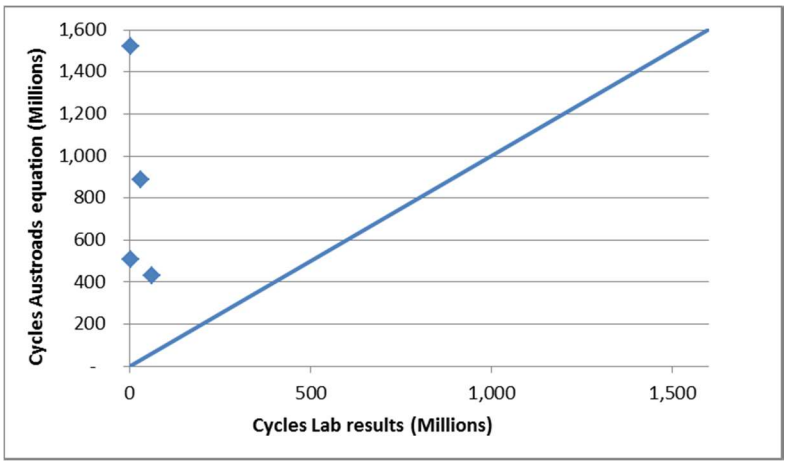

Figure 5-41: Fatigue life from laboratory test against Austroads fatigue equation for slab 2

As it is apparent from Figure 5-40 and Figure 5-41 the estimated fatigue lives from the laboratory are not in line with the determined lives from AGPT02 (Austroads, 2012). This indicates that the AGPT02 fatigue equation should be reviewed for foam bitumen stabilised material.

6. SUMMARY, CONCLUSION AND RECOMMENDATION

6.1 Summary

This study was carried out to determine fatigue life of foamed bitumen stabilised materials. The main focus of the investigation was placed on evaluating the suitability of AGPT02 asphalt fatigue equation for foamed bitumen stabilised materials. Following is the summary of each chapter:

Chapter one–Introduction:

The study included a review of the literature relevant to the stabilisation of pavement and laboratory testing of Western Australian base course materials.

Chapter two–Literature review:

This chapter included a review of previous works, definition of pavement types, pavement rehabilitation and stabilisation methods, modes of failure of flexible pavements, numerical and experimental investigations, and different approaches used to determine the fatigue life of pavement including the identification of research gaps.

Chapter three–Sample preparation:

This chapter covered sample source and details of testing conducted on the samples. Tests including; binder contents, particle size determination, density and air void.

Chapter four–Testing program and equipment:

The testing program is Included an overview of four-point fatigue test, large beam fatigue test apparatus, UTS18 software, preliminary testing and a definition of validity.

Chapter five–Test results and analysis

Analysis carried on determining fatigue life including curve fitting, using extrapolation on fatigue results, phase angle and Hysteresis loop studies and Austroads fatigue formula evaluation.

Chapter six–Summary, Conclusion and recommendation

A summary of findings and conclusion is presented and some recommendations for further research are included in this chapter.

6.2 Conclusion

The following conclusions have been made at the completion of this investigation:

- A logarithmic equation for fatigue curve fitting can be adopted for each sample using different fitting parameters.
- As explained, the majority of the tests have not met the termination condition. For this reason, the fatigue life extrapolated using fitted curve.
- By comparing phase lags for 2 Slabs, the concept that adding more bitumen as viscous additive results in viscoelastic performance of the material was confirmed.
- It was confirmed that the dissipated energy values are higher when the flexural stiffness of bigger. The reason is a bigger force should be applied to the beams to maintain the constant strain during four-point bending beam testing which results in higher dissipated energy for each loading cycle.
- Experimental results of this study show that the AGPT02 (Austroads 2012) formula currently employed for asphalt fatigue life determination is not reliable for foam bitumen stabilised materials.

6.3 Recommendation

The large beam testing programme has shown some variables in the performance of the material, some of which cannot be explained with the limited database available at present hence more research and care is recommended with the use of a current AGPT02 fatigue equation for foamed bitumen stabilised material. Based on this study's investigation results and conclusions the following recommendations are suggested;

- More research into an Austroad's fatigue equation should be undertaken to find more appropriate fatigue equation to allow more confident designs.
- Expand the research to different types of material.
- Carry out testing with both large and standard beams to determine if there is any correlation between the results using different size of samples. Based on Alderson's report material from Nicholson Road would be expected to be the least fatigue resistant using standard fatigue test at strain levels above 85με.(Alderson Allan, 2002). However,

results from large beam test using strain levels above 85με shows very long fatigue life for this material.

- Additional effort/measures and user controls are recommended to reduce test inconsistencies is desirable for future large beam fatigue testing.
- The temperature was set to 20 degrees for all samples. It is recommended to repeat more tests in different temperature to see if the life will improve in higher temperature.
- The frequency of 5Hz was used in all the tests conducted on slab 2 to reduce the failure. It is recommended to do a rigorous study on the effect of rate of loading.

7. REFERENCES

AASHTO, 2008. *Mechanistic-empirical pavement design guide, interim edition: a manual of practice.* Washington, DC: American Association of State and Highway Transportation Officials.

Adlinge, S. S. & Gupta, A. K., 2013. Pavement Deterioration and its Causes. *IOSR Journal of Mechanical & Civil Engineering (IOSR-JMCE),* pp. 9-15.

Alderson, A., 2000. *Fatigue Properties of Bitumen/Lime Stabilised Materials - Interim Report,* s.l.: ARRB Transport Research Ltd.

Alderson, A., 2001. *Ancillary information: Fatigue properties of bitumen/lime stabilised materials,* Canning: ARRB.

Alderson, A., 2002. *Fatigue properties of foamed stabilised materials - Stage 3,* Canning: ARRB Transport ResearchLtd..

Al-Khateeb, G., 2008. Fatigue Performance. *Canadian Journal of transportation,* p. Figure 3.

Al-Khateeb, G., 2008. Fatigue Performance: Asphalt Binders versus Mixtures versus Full-Scale Pavements. *Canadian Journal of Transportation,* pp. Vol 2, No 1.

ARRB, 2013. *Pavements and Materials.* [Online]
Available at: http://www.arrb.com.au/Infrastructure/Pavements-materials.aspx
[Accessed 20 May 2013].

Artamendi, I. & Khalid, H., 2013. *Different approches to depict fatigue of bitumous materials ,* Liverpool: Dept. of Civil Engineering, University of Liverpool.

Asadi, H., 2015. *Experimental modelling for flexible pavement materials applying advanced laboratory tests to develop Mechanistic-Empirical design procedure,* Perth: Curtin University.

Asadi, H., Leek, C. & Nikraz, H., 2013. *Effect of temperature on fatigue life of asphalt.* Brisbane, Royal International Conference Centre.

Aure, T. & Ioannides, A., 2012. Numerical analysis of fracture process in pavement. *Canadian Journal of Civil Engineering, Vol. 39, No. 5,* pp. 506-514.

Austroads, 1996. *Performance of Unbound and Stabilised Pavement Materials under Accelerated Loading.* Sydney, NSW: s.n.

Austroads, 1998. *Guide to Stabilisation in Roadworks.* Sydney, NSW: Austroads Inc..

Austroads, 2005. *Guide to Pavement Technology Part 1: Introduction to Pavement Technology.* Sydney, NSW.: Austroads Inc..

Austroads, 2006. *Guide to Pavement Technology Part 4D: Stabilised Materials.* Sydney, NSW.: Austroads Inc..

Austroads, 2008. *Guide to Pavement Technology Part 2: Pavement Structural Design.* Sydney, NSW: Austroads Inc.

Austroads, 2008. *Guide to Pavement Technology Part 4: Pavement Materials.* Sydney, NSW: Austroads Inc.

Austroads, 2012. *Austroads Guide to pavement technology part 2: pavement structural design.* Sidney, NSW: Austroads Inc..

AustStab, 2007. *Technical note 3, Stabilisation using insoluble dry powdered polymers.* [Online]
Available at: www.auststab.com.au
[Accessed 21 05 2013].

AustStab, 2008. *AustStab Technical Note No.2F Foamed bitumen stabilisation.* [Online]
Available at: www.auststab.com.au
[Accessed 21 May 2013].

Baburamani, 1999. *Asphalt fatigue life prediction models – a literature review,* s.l.: ARRB research report, ARR no. 334.

Bocz, P., 2009. Pre-Assumption of Final Results of the Asphalt Four-Point Flexing-Beam Fatigue Test. *Acta Technica Jaurinensis,* Volume 2, pp. 107-115.

Browne, A., 2015. *Hiway stabilizers.* [Online]
Available at: http://www.hiwaystabilizers.co.nz/media/16458/fbr_in_nz.pdf
[Accessed 26 03 2015].

Buttlar, W. G., Paulino, G. H. & Song, H. S., 2006. Application of Graded Finite Elements Application of Graded Finite Elements. *Journal of engineering mechanics,* pp. 240-249.

Das, A., 2008. *Principles of bituminous pavement design and the recent trends,* Kanpur: University Of IITK.

ELLPAG, 2006. Long-life pavements. *International Journal of Pavement Engineering.*

Experiment-resources, 2015. *www.experiment-resources.com.* [Online]
Available at: www.experiment-resources.com
[Accessed 15 01 2015].

Government, A., 2009. *2006-7 Local Government National Report,* Canberra: Australian Government, Department of infrastructure, Transport, Regional Development and Local Government.

Harvey, J. T., Deacon, J. A., Tsai, B.-W. & Monismith, C. L., 1995. *Fatigue performance of asphalt concrete mixes and its relationship to asphalt concrete pavement performance in California,* Berkeley USA: University of California.

Huan, Y., 2014. *Effects of Aggregate Properties on Strength Characteristics of the Foamed Bitumen Mixture with Relation to WesternAustralian Roadway Construction,* s.l.: Curtin University.

Interactive, P., 2007. *Pavement management.* [Online]
Available at: http://www.pavementinteractive.org/article/fatigue-cracking/
[Accessed 12 07 2015].

Jenkins, K. J., Van de Ven, M. F. & de Groot, J. L., 1999. *Characterisation of Foamed Bitumen.* s.l., s.n.

Kendall, M., Baker, B., Evans, P. & Ramanujam., J., 1999. Foamed Bitumen Stabilisation. *Foamed Bitumen Stabilisation – Southern Region Symposium,* p. 2.

Leek, C., 2002. *Performance Characteristics of insitu foamed bitumen stabilised Pavements,* Canning: City of Canning Western Australia.

Leek, C., 2013. *Fatigue and dynamic modulus* [Interview] (5 10 2013).

Leek, C., Nikraz, H. & Chegenizadeh, A., 2014. Engineering characterisation of in situ foamed bitumen stabilised pavements. *Australian Geomechanics,* Volume 49, pp. 133-142.

Main-Roads-WA, 2013. Regional Road Length Statistics, Road Information Services. *Regional Road Length Statistics*, August.

Muthen, K. M., 1998. *Foamed Asphalt Mixes Mix Design Procedure,* Pretoria, South Africa: CSIR Transportek.

Nejad, F., Notash, M. & Forough, S., 2015. Evaluation of Healing Potential in Unmodified and SBS-Modified Asphalt Mixtures Using a Dissipated-Energy Approach. *Journal of Materials in Civil Engineering.*

Pavementinteractive, 2011. *Pavement.* [Online]
Available at: http://www.pavementinteractive.org/category/pavement/
[Accessed 15 December 2011].

Pell, P., 1962. *Fatigue characteristics of bitumen and bituminous mixes.* Ann Arbor, Michigan, s.n.

Priest, A. L. & Timm, D. H., 2006. *Methodology and calibration of fatigue transfer functions for mechanistic-empirical flexible pavement design,* Alabama: NCAT.

Queensland Department of Transport and Main Roads Pavements, M. &. G. B., 2012. *Pavement rehabiliation manual,* s.l.: Queensland Department of Transport and Main Roads.

Ramanujam, J. M. & Jones, J. D., 2000. *characterisation of foamed bitumen stabilisation,* s.l.: AustStab.

Shell, 1978. *Shell pavement design manual: asphalt pavement and overlays for road traffic.* London, UK: Shell International Petroleum.

Shen, S. & Carpenter, S., 2007. *An energy approach for airport pavement low damage.* Atlantic City, New Jersey, USA, s.n.

Souliman, M., 2012. *Assessment of different flexure fatigue failure analysis methods to estimate the number of cycles to failure of asphalt mixtures.* Nevada, 3rd 4PBB Conference.

Stubbs, A. P., 2011. *Fatigue Behaviour of Hot Mix Asphalt for New Zealand Pavement Design,* s.l.: University of Canterbury.

Sunarjono, S., 2013. *Performance of Foamed Asphalt under Repeated Load Axial Test.* Surakarta, Indonesia, Procedia Engineering, pp. 698-710.

Van Dijk, W. & Visser, W., 1997. The energy approach to fatigue for pavement design. *Proceedings Assoication of Asphalt Paving Technologists, 46,* pp. 1-40.

White, G., 2006. *Laboratory Characterisation of Cementitiously Stabilised Pavement Materials,* Sydney: Master of Engineering, School of Aerospace, Civil and Mechanical Engineering, University of New South Wales.

Wilmot, T. D., 1991. *The recycling opportunities in the effective management of road pavements.* s.l., s.n.

Wilmot, T. & Vorobieff, G., 1997. *Is Road Recycling A Good Community Policy.* s.l., Australian Stabilisation Industry Association.

YU, H., 2012. *Design and characterization of asphalt mixtures based on particle packing and mechanical modeling,* s.l.: Washington State University, Department of Civil and Environmental Engineering.

8. APPENDIX A–UTS18'S FOUR POINT TESTING RESULTS FOR ALL THE SAMPLE

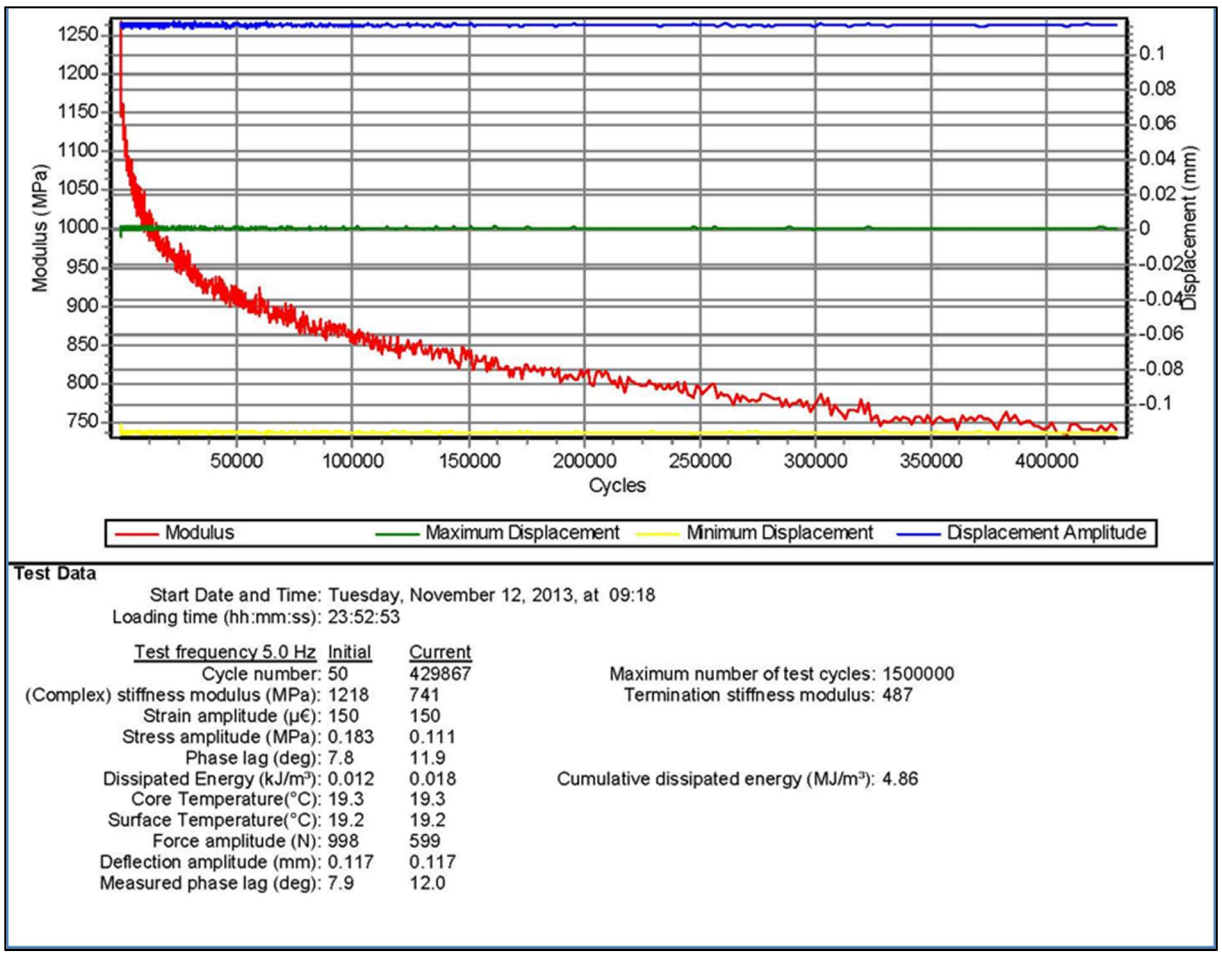

Figure 8-1: Testing issues and outcomes for Sample number 1

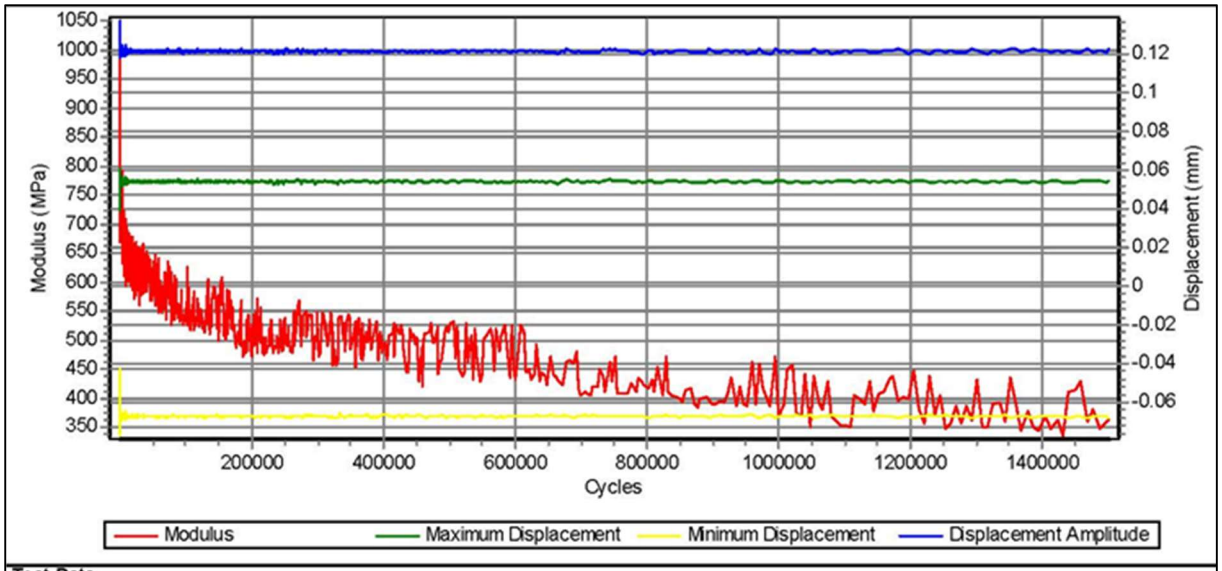

Test Data

Start Date and Time: Wednesday, November 20, 2013, at 09:47
Loading time (hh:mm:ss): 41:40:00

Test frequency 10.0 Hz	Initial	Current	
Cycle number:	50	1500000	Maximum number of test cycles: 1500000
(Complex) stiffness modulus (MPa):	738	362	Termination stiffness modulus: 295
Strain amplitude (με):	149	151	
Stress amplitude (MPa):	0.110	0.055	
Phase lag (deg):	-0.4	13.3	
Dissipated Energy (kJ/m³):	0.000	0.013	Cumulative dissipated energy (MJ/m³): 10.97
Core Temperature(°C):	19.2	19.2	
Surface Temperature(°C):	19.2	19.1	
Force amplitude (N):	580	299	
Deflection amplitude (mm):	0.120	0.122	
Measured phase lag (deg):	179.7	14.9	

Figure 8-2: Testing issues and outcomes for Sample number 2

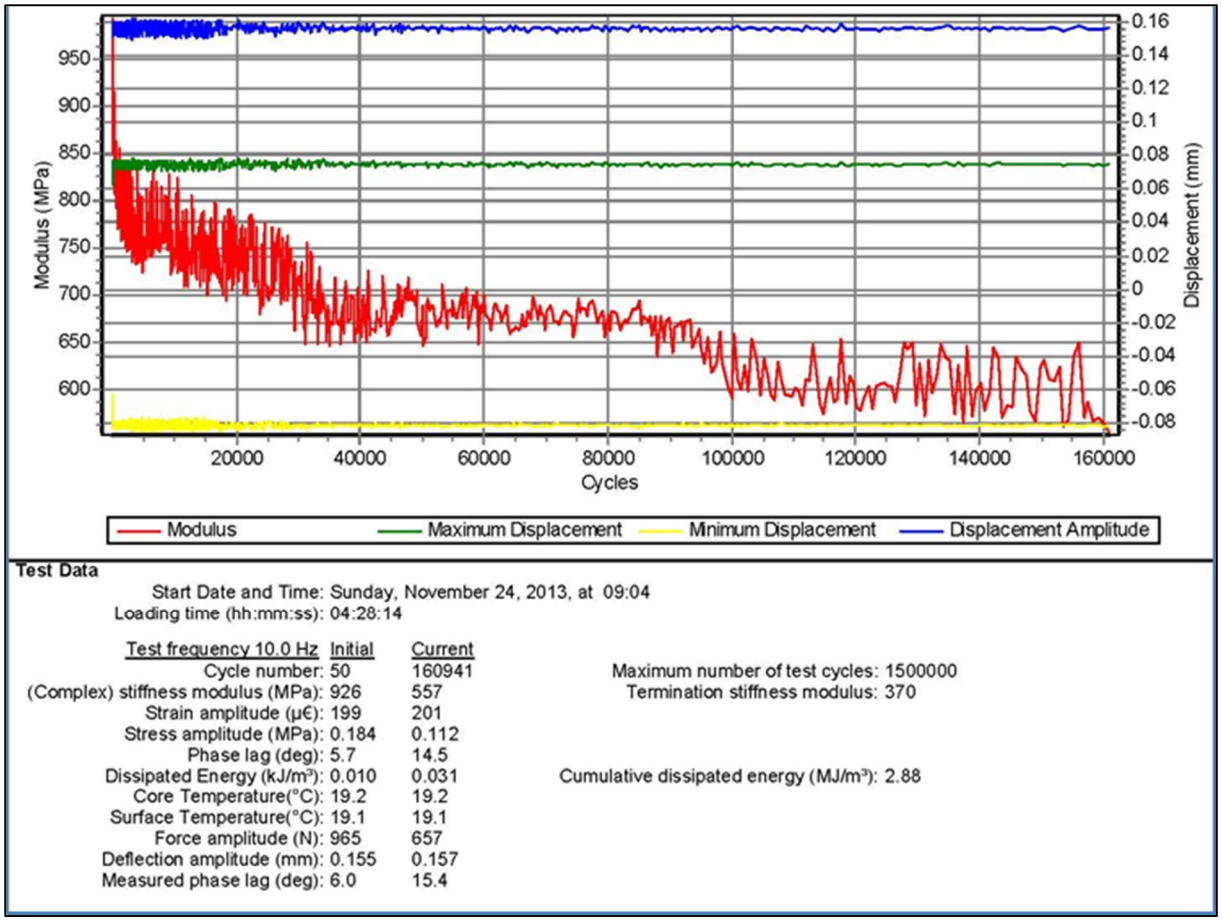

Figure 8-3: Testing issues and outcomes for Sample number 4

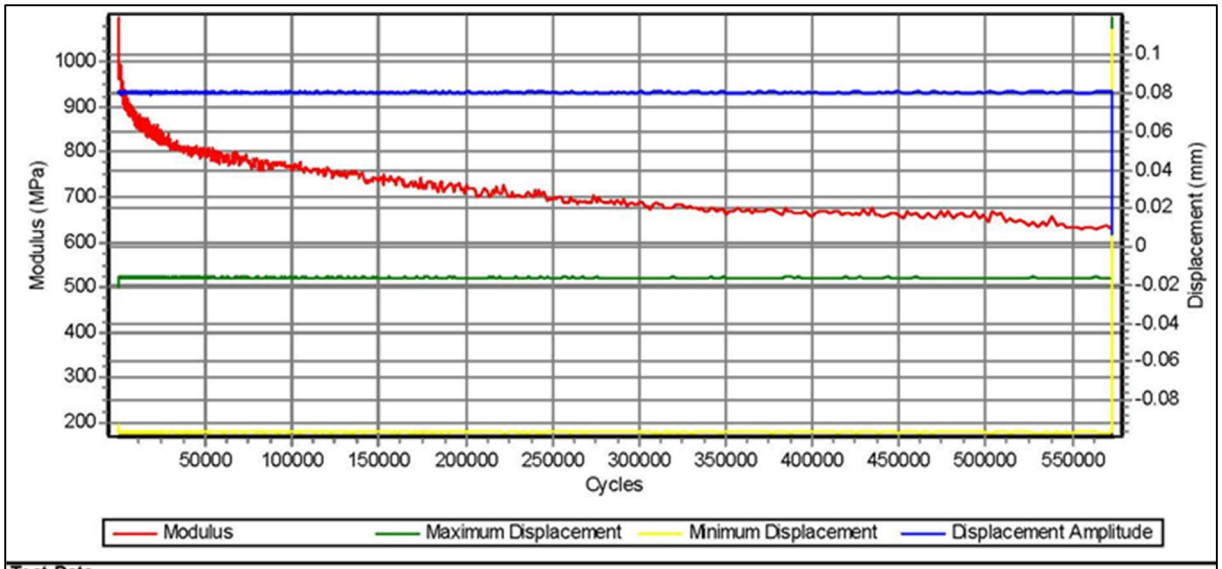

Test Data

Start Date and Time: Thursday, March 13, 2014, at 15:19
Loading time (hh:mm:ss): 31:49:26

Test frequency 5.0 Hz	Initial	Current
Cycle number:	50	572831
(Complex) stiffness modulus (MPa):	1054	176
Strain amplitude (μ€):	100	8
Stress amplitude (MPa):	0.105	0.001
Phase lag (deg):	-12.2	-11.8
Dissipated Energy (kJ/m³):	0.007	0.000
Core Temperature(°C):	19.1	19.2
Surface Temperature(°C):	19.0	19.1
Force amplitude (N):	533	6
Deflection amplitude (mm):	0.080	0.006
Measured phase lag (deg):	167.9	169.0

Maximum number of test cycles: 1500000
Termination stiffness modulus: 422

Cumulative dissipated energy (MJ/m³): 5.29

Figure 8-4: Testing issues and outcomes for Sample number 8

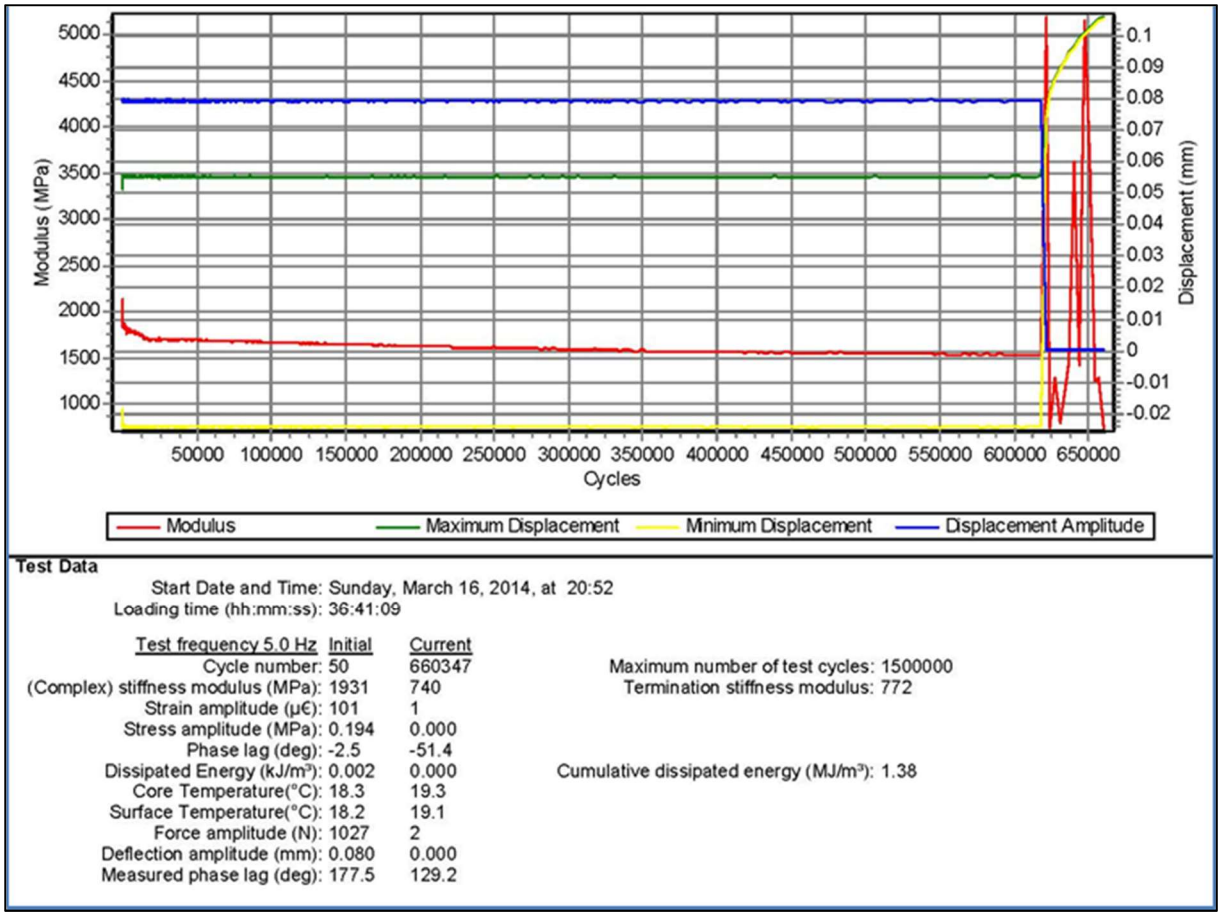

Figure 8-5: Testing issues and outcomes for Sample number 9

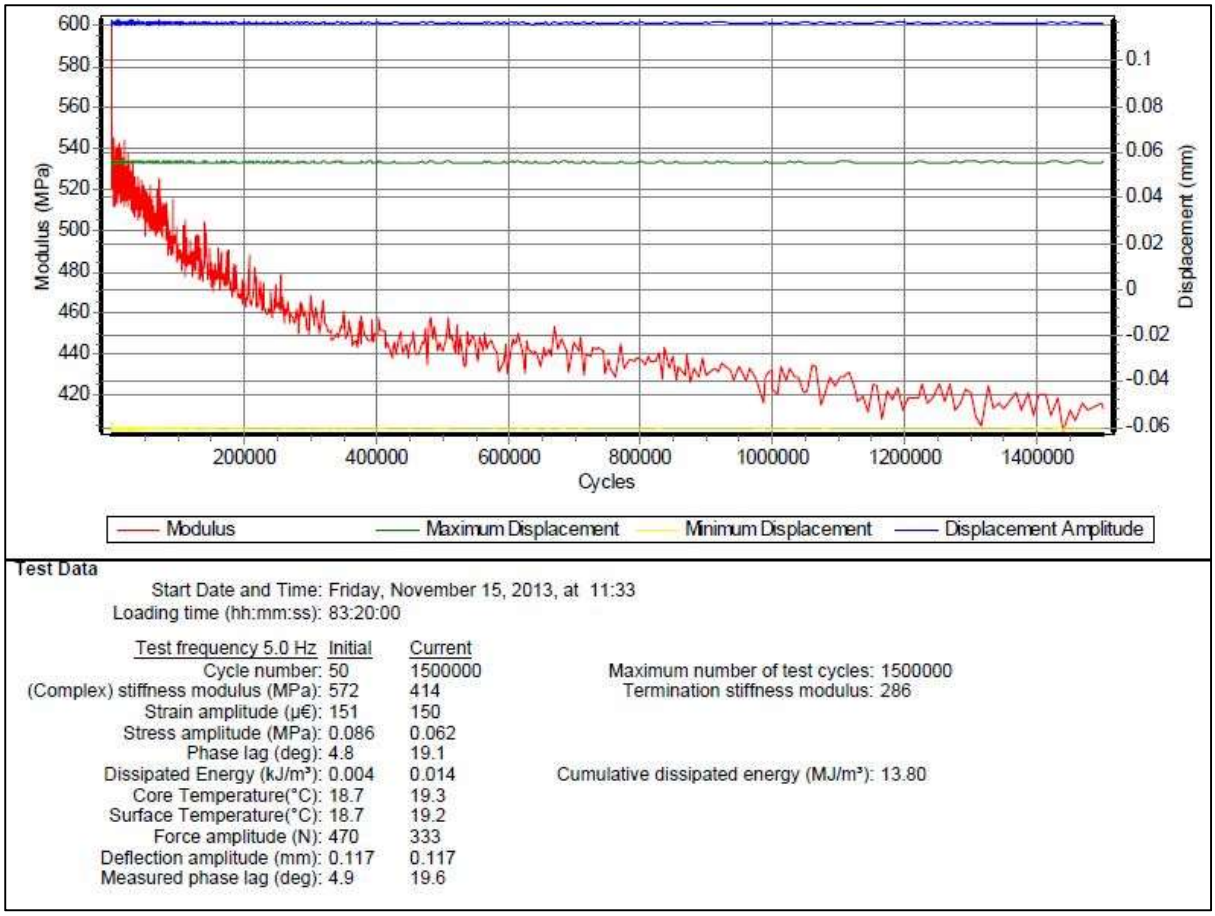

Test Data

Start Date and Time: Friday, November 15, 2013, at 11:33
Loading time (hh:mm:ss): 83:20:00

Test frequency 5.0 Hz	Initial	Current	
Cycle number:	50	1500000	Maximum number of test cycles: 1500000
(Complex) stiffness modulus (MPa):	572	414	Termination stiffness modulus: 286
Strain amplitude (µ€):	151	150	
Stress amplitude (MPa):	0.086	0.062	
Phase lag (deg):	4.8	19.1	
Dissipated Energy (kJ/m³):	0.004	0.014	Cumulative dissipated energy (MJ/m³): 13.80
Core Temperature(°C):	18.7	19.3	
Surface Temperature(°C):	18.7	19.2	
Force amplitude (N):	470	333	
Deflection amplitude (mm):	0.117	0.117	
Measured phase lag (deg):	4.9	19.6	

Figure 8-6: Testing issues and outcomes for Sample number 10

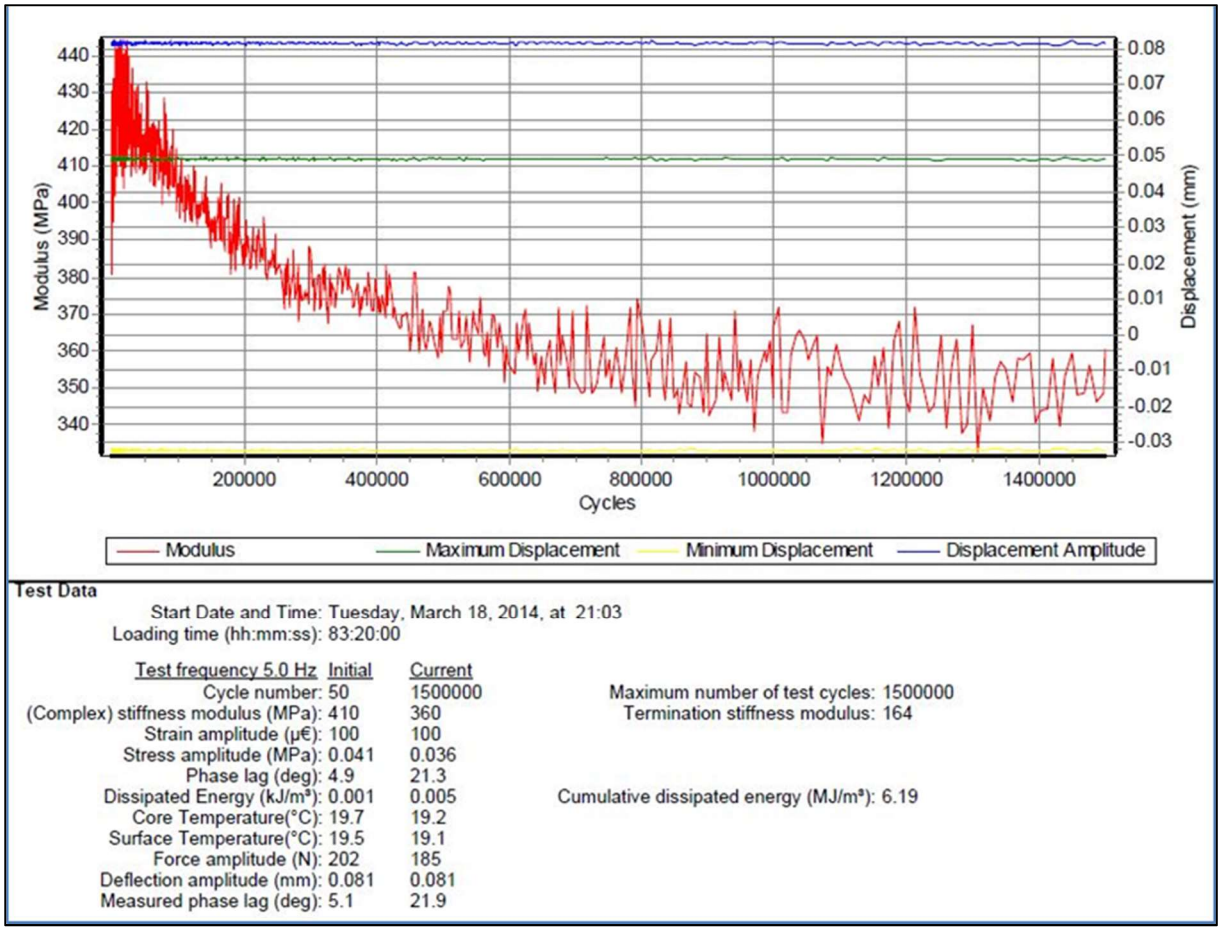

Figure 8-7: Testing issues and outcomes for Sample number 11

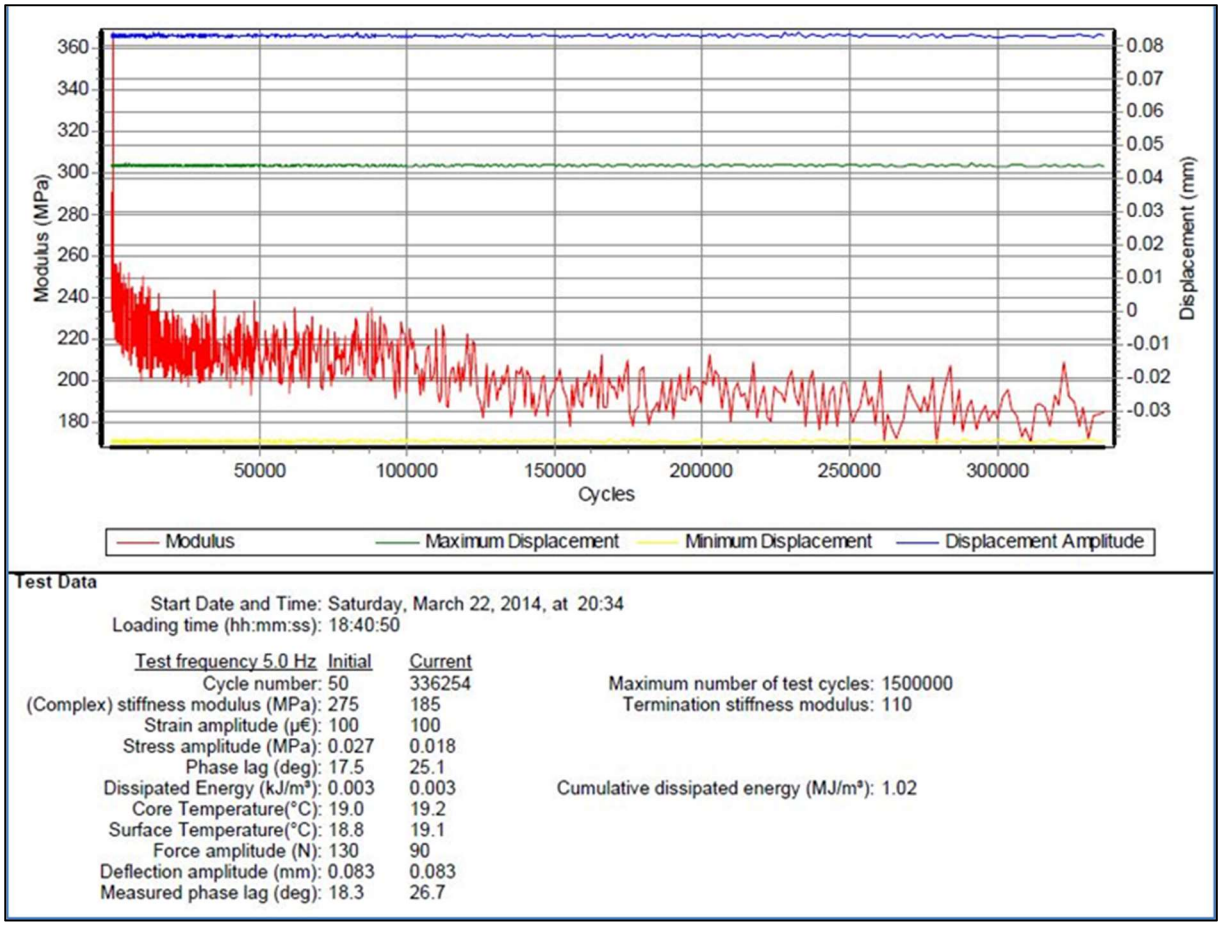

Test Data

Start Date and Time: Saturday, March 22, 2014, at 20:34
Loading time (hh:mm:ss): 18:40:50

Test frequency 5.0 Hz	Initial	Current
Cycle number:	50	336254
(Complex) stiffness modulus (MPa):	275	185
Strain amplitude (μ€):	100	100
Stress amplitude (MPa):	0.027	0.018
Phase lag (deg):	17.5	25.1
Dissipated Energy (kJ/m³):	0.003	0.003
Core Temperature(°C):	19.0	19.2
Surface Temperature(°C):	18.8	19.1
Force amplitude (N):	130	90
Deflection amplitude (mm):	0.083	0.083
Measured phase lag (deg):	18.3	26.7

Maximum number of test cycles: 1500000
Termination stiffness modulus: 110

Cumulative dissipated energy (MJ/m³): 1.02

Figure 8-8: Testing issues and outcomes for Sample number 12

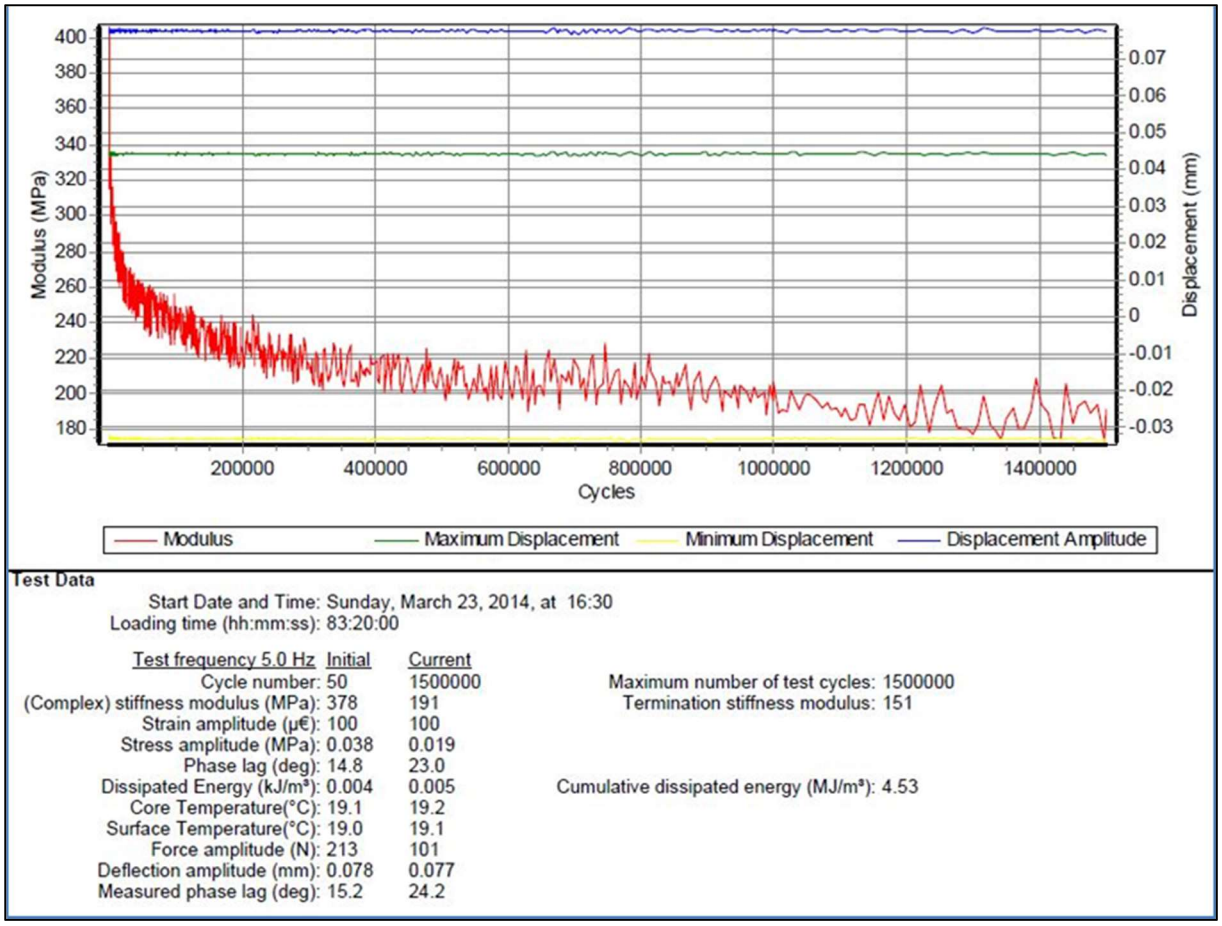

Test Data

Start Date and Time: Sunday, March 23, 2014, at 16:30
Loading time (hh:mm:ss): 83:20:00

Test frequency 5.0 Hz	Initial	Current	
Cycle number:	50	1500000	Maximum number of test cycles: 1500000
(Complex) stiffness modulus (MPa):	378	191	Termination stiffness modulus: 151
Strain amplitude (µ€):	100	100	
Stress amplitude (MPa):	0.038	0.019	
Phase lag (deg):	14.8	23.0	
Dissipated Energy (kJ/m³):	0.004	0.005	Cumulative dissipated energy (MJ/m³): 4.53
Core Temperature(°C):	19.1	19.2	
Surface Temperature(°C):	19.0	19.1	
Force amplitude (N):	213	101	
Deflection amplitude (mm):	0.078	0.077	
Measured phase lag (deg):	15.2	24.2	

Figure 8-9: Testing issues and outcomes for Sample number 13

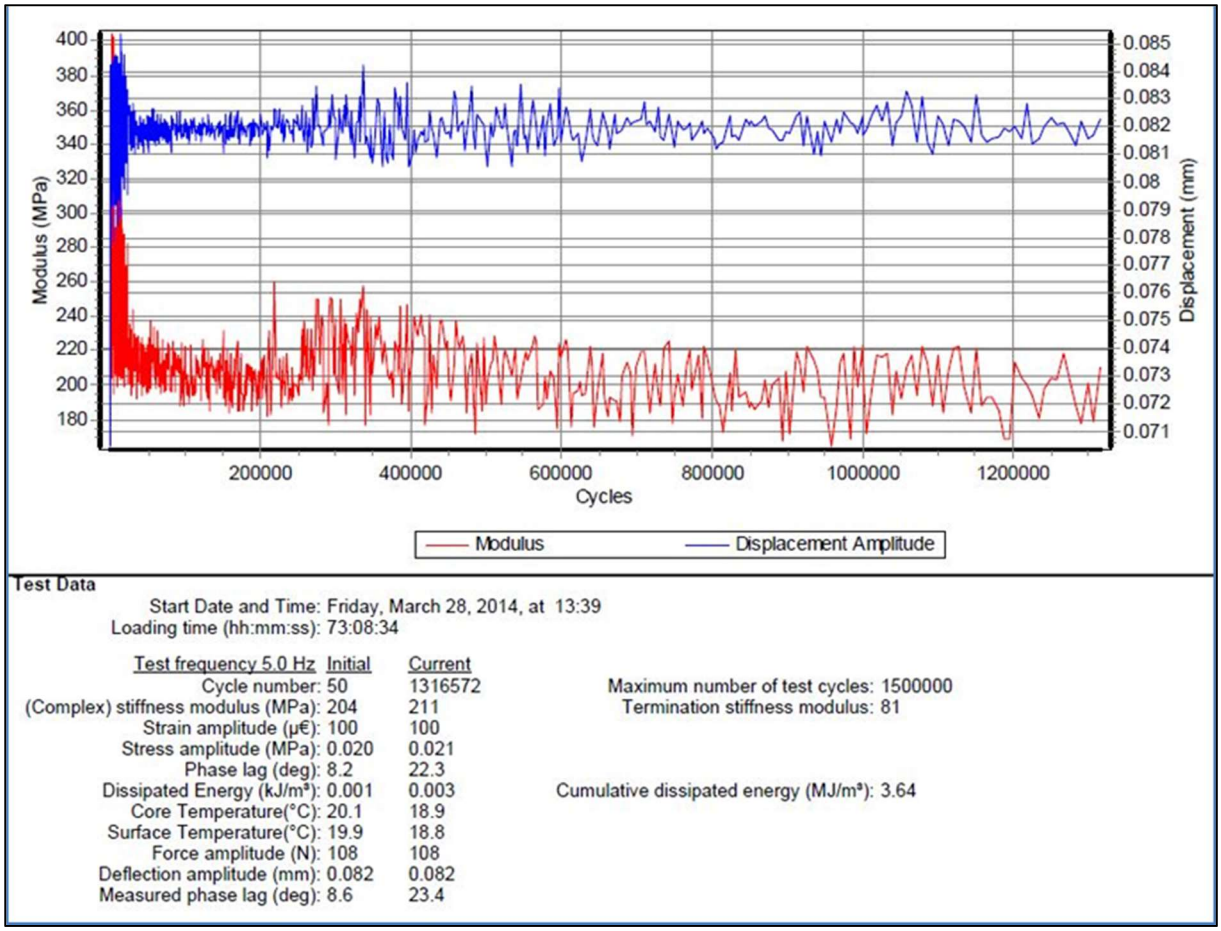

Figure 8-10: Testing issues and outcomes for Sample number 14